UNIVERSITÀ DEGLI STUDI DI PADOVA

DIPARTIMENTO DI TECNICA E GESTIONE DEI SISTEMI INDUSTRIALI

Department Of Management and Engineering

Corso di Laurea Magistrale in Ingegneria dell'Innovazione del Prodotto

Tesi di Laurea Magistrale

Material Characterization and Finite Element simulation of Ice Hockey Helmets under rotational impact conditions

Relatore: Ch.mo PROF. Nicola Petrone

Relatore: Ch.mo PROF. Svein Kleiven, KTH Stockholm

Correlatore: Madelen Fahlstedt, KTH Stockholm

Laureando: Stefano Civin

ANNO ACCADEMICO. 2017/2018

Abstract

The present work is developed at the Royal Institute of Technology (KTH) in Stockholm, Sweden under the supervision of Prof. Svein Kleiven and Madelen Fahlstedt and at the University of Padova under the supervision of Prof. Nicola Petrone.

The aim is to improve a finite element model of an Ice Hockey helmet generated in 2017 by I. Rigoni [1], by mean of an extended material characterization and material model validation of the EPP foam liner.

To characterize the material a new shear test rig is designed and builtin order to fit the samples of the convenient size: it is often required to test samples directly extracted from commercial helmets and a suitable specimen size must be chosen to be able to cut the samples from such a complex shaped part which an helmet liner is.

The material data obtained fom the test (Compression, Tension, Shear) are used to prepare a MAT_083 Fu Chang foam material card in LS-PrePost to be implemented in the LS-Dyna simulation of the helmet oblique impact test previously performed at MIPS (Sweden).

The material model is tuned and validated in compression and shear for two different strain rates, but the model demonstrated to overestimate the kinematic parameters of the hit.

An alternative MAT_057 Low Density Foam material model is tested with slightly better results, using the same data, not accounting for strain rate dependence.

Five configurations are proposed with changes in the material model and in the fitting of the head/helmet system. The non fitted configuration were better correlating the results with all the material models. The tuning of the material to match the shear response with the experimental one gave a very small contribution.

Index

Introduction

At KTH Neuronic Department, a large portion of the research activity is focused on the analysis and finite element simulation of accidents. The covered fields space from fall injury (related to femur neck fracture in elderly people), winter sport injuries (ex. falling on ski/snowbard), contact sport impact (Football, Hockey, Boxe).

Because of the impossibility to use direct experimental techniques, innovative methods have to be used to be able to correlate the occurring of injuries with paramenter that are able to predict the risk of a brain damage to be caused in a specific situation.

The approach is, on one side based on animals and cadaver experiments, aimed to find relations between the kinematic of the head and the clinical outcome in terms of injury. Experiments on cadavers are used to study the mechanical aspect of an impact, for example by mean of the insertion of targets inside the brain and monitoring of strains using motion tracking techniques in x-ray frames of drop tests [2] .

The availability of Finite Element (FE) codes and computing resources, allowed researchers to develop FE models of the human head [3] that are constantly being improved. The simulation of an impact performed on a validated head FE model can be used to see what is happening inside the Skull in that specific situation. Accident reconstruction performed from video analysis and with the use of dedicated software allow to determine the kinematic of the actors prior to impact and, evaluate the relation between finite element and clinical outcomes by mean of specific predictors, and evaluate the effectiveness of protective gear [4] . Validation of FE results against MRI on the injured subject confirmed the quality and ability of the combination FE-simulation with Clinical Reports to assess whether and how a brain injury is determined.

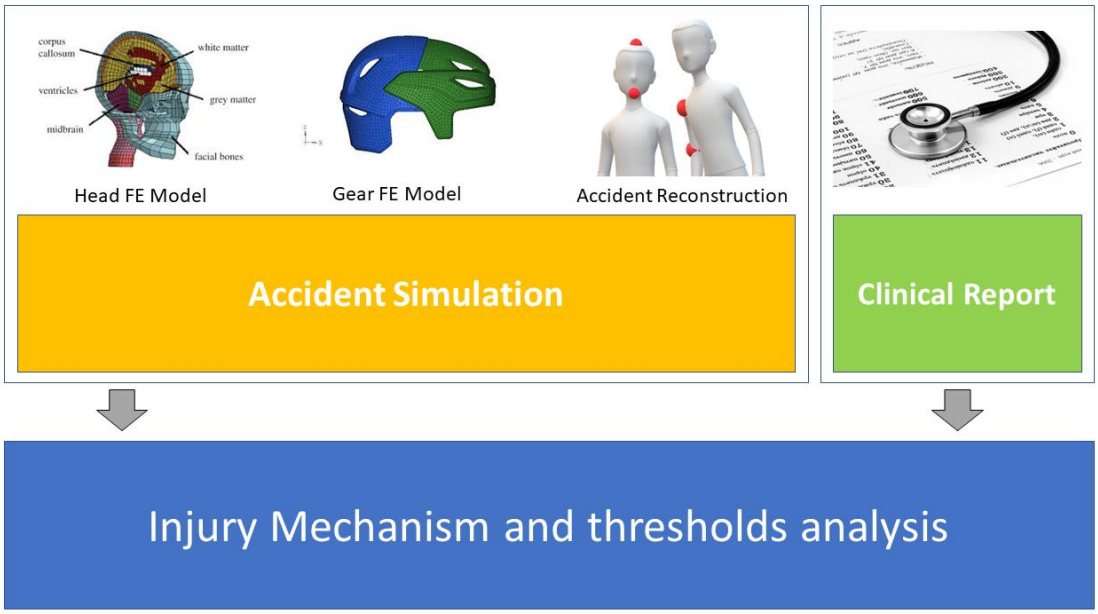

FIGURE 1 WORKFLOF FOR ACCIDENT RELATED TBI RESARCH

The present work is focused on the development of the FE model of an helmet, to be potentially used in the simulation of Ice Hockey Impacts.

Since to the rotational kinematics is recognized an inportant role in the level of axonal strain, the oblique impact testing and simulation of the protective effect of the helmets became an importan area of investigation, although the present helmets test standards don't require an oblique impact testing to evaluate the head rotational kinematic.

Since the material of the liner undergoes severe shear deformation it is necessary to have a correct material characterization to perform reliable finite element analysis, for this reason a shear test rig and material validation are performed.

Brain Injuries in Ice Hockey

In the USA a number of 1.7 Billion (per Year) of TBI is estimated, 20% of which happens during sports activity (source: https://www.statisticbrain.com).

TBI can be of various severity, the less severe injuries are named Mild Traumatic Brain Injury (MTBI), one of the most common types of MTBI is concussion (42% of all Ice Hockey injuries [5]). Concussion is defined as a brain injury caused by the rapid movement of the brain inside the cranium, causing disruption of the brain cell function.

To be specific, referring to concussion, the sport with higher incidence is Cycling, and among the team sports Hockey and Football are on top of the raking. Several studies were performed to assess incidence rates and the relevant trends during the years. It is in general noticeable an increase in the injury rate in the recent season, and an increase in the severity of the brain injuries. This can be related to a general increase of the player's velocity on the ground, due to the evolution of the equipment and of the athletes conditioning. Also, a general increase in the compulsory protection that players are wearing can indirectly make them less sensible to the risk of impacting because of the higher perceived protection.

To reduce the occurrence of TBI new rules have been implemented in ice hockey, for example the #48 in the NHL that eliminates head targeted body checks, but the TBI rate has steadily increased over the last seasons, and Ice Hockey remains the sport with the highest concussion rate among young players.

It is important to note that MTBI are critical for players because they are often underestimated in the magnitude, and poorly treated. MTBI are associated with a list of possible immediate symptoms, such as headache, vomiting, dizziness, sensitivity to light and sound. In the occurrence of one of more sign of concussion usually a rest period is prescribed, and the return to play time is conditioned by the time that it takes for the player to be asymptomatic, and for the history of the specific player, after the first MTBI the rest time is increased and in some cases the activity must be stopped.

Very often this kind of treatment is effective in the short-term, but it is recognized that MTBI can have delayed symptoms, such as memory loss or psychiatric disorders that could affect the subject life.

For these reason official sport leagues are promoting the research on the brain's biomechanics and on the equipment design, through funding and collaboration within universities, research centers and companies. Effort is being put in the understanding of the brain damage mechanism, on the accident reconstruction and in the protection device design.

Brain damage mechanism

The MTBI can be predicted in a good way using mechanical parameters, for example accelerations, translational and rotational, and strain of the brain matter. By mean of the use of refined anisotropic Finite Element Models of the human head [3] and NFL accident reconstruction, it was found that axonal strain is a good predictor for the occurrence of MTBI [6]. To be

Due to the mechanical properties of the brain tissue, that have a bulk modulus five to six orders of magnitude higher than the shear modulus, rotational accelerations are associated with higher strains and thus with higher severity of the brain injury. It is possible to state that traumatic brain injuries due to axonal strain are caused by rotational accelerations, while skull fractures are mostly related to translational acceleration. [7]

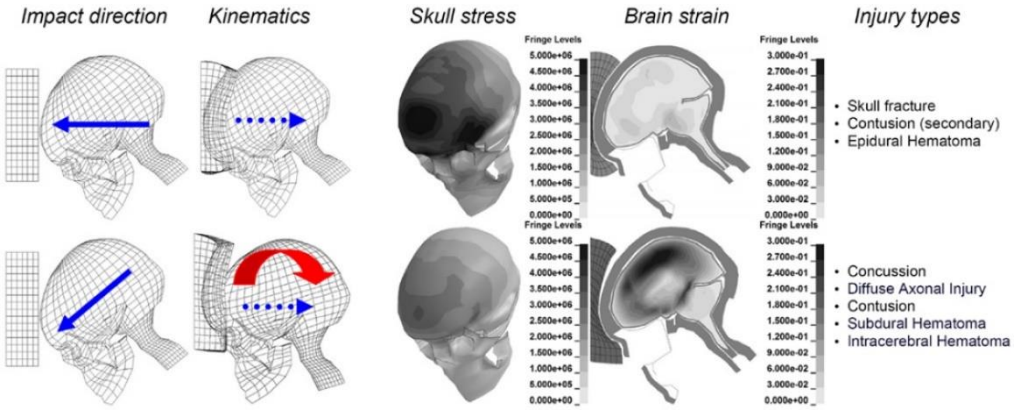

FIGURE 2 EFFECT OF DIFFERENT IMPACT DIRECTION (SVEIN KLEIVEN, 2013)

Kinematic parameters of interest

As explained in appendix A, where the main injury criterions are briefly described, the main kinematic parameters are the translational acceleration, rotational acceleration, rotational velocity and their value within time as explained in Appendix A Head Injury Criterions. The direction of the acceleration is also influent as explained in the BrIC Brain Injury Criterion [28]

Helmet design standards and testing

In the case of helmet design and certification the test procedure changes from type to type of helmet, involving different test in reason of the actual risks the users are subjected to. In general, the test standards provide limitation on the accelerations (during drop tests or under impactor loading), penetration resistance (ex. Climbing helmets), covering of specific areas (es. Ice hockey helmets).

Ice hockey helmet test standards

For Ice Hockey helmets the ASTM F1045-16, *Standard Performance Specification for Ice Hockey Helmets* [8] is the reference.

The prescriptions refer to shock absorption properties, strength and elongation of the chin strap (retention system), area of coverage and penetration resistance. Also, prescriptions on materials, distortion at high/low temperatures, sharp edges and rivets are present.

For Ice Hockey helmets, the drop tests are carried on at least 4 helmets for each size, that are going to be tested under different conditions:

- Two helmets at ambient conditioning, one with prescribed impact points, the other with free impact point (two)
- One Cold conditioned helmet (from 4h to 24h at a temperature between -27°C and -23°C)
- One hot conditioned helmet (from 4h to 24h at a temperature between 28°C and 32°C).

The conditioned helmets are tested under impact on the two points that yielded the highest max acceleration values in the ambient conditioned samples.

The impact velocity must be 4.5 m/s ± 0.1 m/s.

The parameter that must be reported are, for each impact:

- The maximum acceleration, in g (275 g pass/fail)
- The duration of the impact, defined as the width of the pulse along the 50 g line in milliseconds
- The oscillogram (acceleration – time curves).

Drop test apparatus

The drop test is conducted by mean of dropping an instrumented head form wearing the helmet under the manufacturer specifications onto an anvil.

The structure is constituted by a rail system, that can be made by hard rails or wires (in this case the wires tension prescribed as a minimum of 845N). Along the rail a carriage is free to move in the vertical direction and is possible to control the instant and height at which the fall begin.

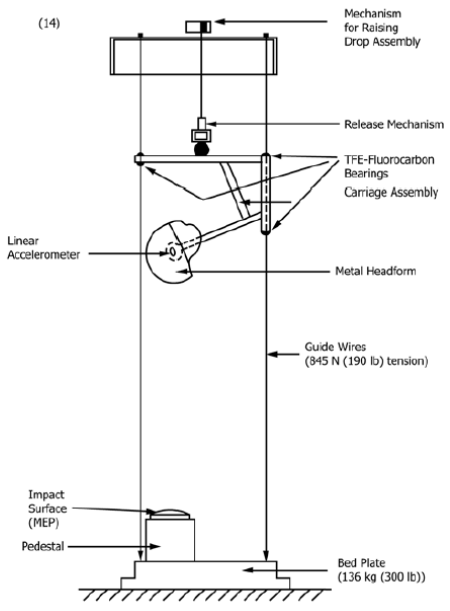

NOTE 1—Rail-guided drop assemblies are also permissible.

FIGURE 3 HELMET DROP TEST RIG (ASTM F1045)

The anvil is flat and located on a robust concrete basement. Over the flat anvil, referring to the previously cited ASTM F1045-16 a Modular Elastomer Programmer (MEP) with prescribed hardness must be present, and used for the system calibration.

Oblique impact test rig.

To perform.the oblique impact tests, that will be simulated in the following, an innovative drop test method on a steel anvil with inclined surface is used [9]. In the picture below a stripe of sand paper is used to provide additional friction with respect to the plain steel surface.

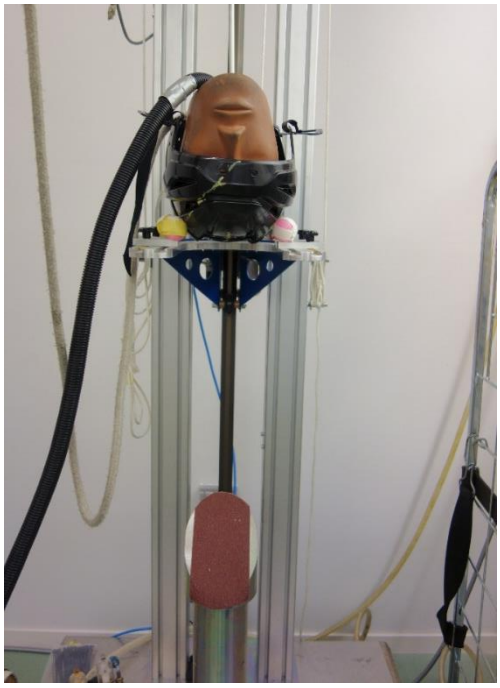

FIGURE 4 OBLIQUE IMPACT TEST RIG (KTH NEURONIC)

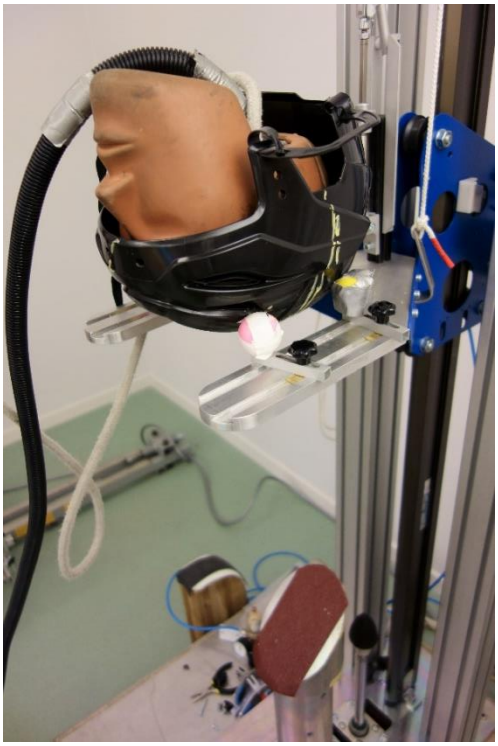

FIGURE 5 HELMET ON OBLIQUE IMPACT TEST RIG (KTH NEURONIC)

The head form is instrumented with an accelerometer located in the Center Of Mass (COM) and can record acceleration data up to 500g with a precision of ±5%. The frequency response must cover the range 5Hz to 900 Hz (variation ±1.5%).

Previous work

In 2017 Isotta Rigoni developed a first FE model of the helmet in question [1].

The material characterization was performed on samples directly extracted from the helmet, with the aim to characterize the properties of the foam extracted from different locations within the liner, and then find an average value. The characterization was performed only on the EPP foam in compression at a maximum strain rate of 10 s^{-1}.

The mesh was generated in Hypermesh® 2017 Student Edition with a final check on the quality.

The FE model was proposed in two configuration, implementing different material models, 063_CRUSHABLE_FOAM and 126_MODIFIED_HONEYCOMB. The first gave discrete results while the second was less reliable.

The major limitations of that study were the material characterization and the material modeling, together with the contact definition. To be specific, the shear properties implemented in the honeycomb were taken from another material (EPS) and not directly tested. The low number of samples in compression and the presence of penetration between foam liner and shell in the FE model are the main area of improvement on which this work is focused.

Chapter 1 Material Characterization

In the following chapter the characterization of the foam Liner material of the helmet is described. The FE model developed in this work consider a bi-material helmet, composed by the Shell, in Acrylonitrile Butadiene Styrene (ABS) and a foam liner in Expanded Polypropylene (EPP) of density approx. 54 Kg/m^3.

ABS (Shell)

TABLE 1 ABS MECHANICAL PROPERTIES

ABS mechanical properties [10]		
Density [Kg/m^3]	Young Modulus [Pa]	Poisson's Ratio
1390.00	1.867e+009	0.35

EPP (Liner)

Since there was not enough material available for being directly extracted from an Easton synergy 380 helmet sample, the specimens were extracted from a block provided by MIPS in the person of Peter Halldin. The measured density was 52 kg/m^3, while the nominal was 50 Kg/m^3.

The Performed tests are Compression, Tensile and Shear. Due to limitation in material and equipment it was not possible to strictly follow the ASTM standards prescriptions, custom designed Tensile and Shear test setup have been used, in each section a description of the test setup, results and data treatment is reported.

All the elaboration of the data was performed in Matlab®2018 [11]

Instron® Electropulse E3000

FIGURE 6 INSTRON ELECTROPULSE E300 IN THE KTH NEURONIC LAB.

The machine used to perform the tests is an Instron® Electropulse E3000, equipped with the *dynacell* load cell (±5kN). [12]

TABLE 2 INSTRON E3000 SPECS

Instron Electropulse E3000 specifications [12]	
Dynamic Capacity	±3000 N (±675 lbf)
Static Capacity	±2100 N (±472 lbf)
Stroke	60 mm (2.36 in)
Load Weighing Accuracy	±0.5 % of indicated load or ±0.005 % of load cell capacity, whichever is greater
Daylight Opening	861 mm (34 in) maximum with actuator at mid stroke
Configuration	Twin-column with actuator in upper crosshead
Load Cell	±5 kN Dynacell™

Compression Test

The compressive test is one of the main characterization used to characterize foamed material that undergoes impact loading. The reference standards in the ASTM system is the ASTM-D1621_16. [13]

Test setup

The load was applied by mean of plates that are provided from the manufacturer(accessories code 2840-030) and the test execution was in displacement control at constant engineering strain rate.

FIGURE 7 COMPRESSION TEST SETUP

Since good accuracy was needed to proceed with the extrapolation of higher strain rates by mean of Nagy's equation, 15 samples per each condition has been tested. Due to the difficulties of cutting the material a small difference in the size from one sample to another was observed, always remaining within 2% of the nominal side length. The samples have been randomly mixed after being cut to avoid bias due to the cutting sequence and orientation.

The tested strain rates are 0.01 s^{-1} , 0.1 s^{-1} , 1 s^{-1}, 10 s^{-1}

The displacement law was a ramp at constant velocity until 85% of eng. Strain (17 mm over 20 mm).

Compression results

No Poisson effect is observed, in the following it is assumed to be equal to 0.05 as reported in Previous work [1] .

The results for the first three strain rates are reported in the figure below, the curves show a strain rate influence in the plateau region, instead in the elastic region the response is similar for the different strain rates.

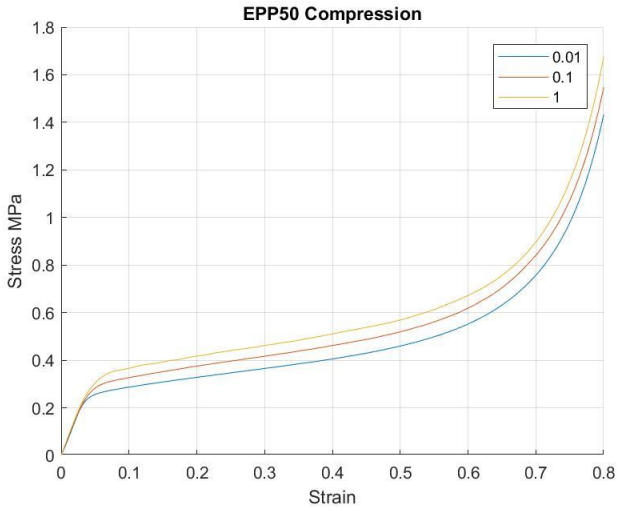

FIGURE 8 EPERIMENTAL COMPRESION CURVES FOR EPP 50

The elastic modulus in Compression has been evaluated in about 7.5 MPa for Strain rate $1s^{-1}$, since this data is used in LS-Dyna only for the calculation of the time-step and contact forces in the solution and the elastic region response can be considered uniform for all strain rates, only this data has been considered.

To generate a set of curves that can ensure stability in the simulation when high strains appear the procedure suggested by Hirth et. Al. [14]

The stress strain curves are extended until 95% of strain, corresponding to the zero-void ratio with an exponential function and then extended until 99% of compression with constant slope corresponding to the elastic modulus of the material (Polypropylene, 2 GPa), resulting in an almost vertical curve. This procedure generate a set of curves that are able to effectively manage high compressive strains without the occurrence of negative volume errors in the Finite Element Model solution.

Although this procedure is reasonable from the physical point of view, in terms of solution time with some material models it can cause a relevant increase, in the following part regarding the material model choice an explanation and solution is proposed.

Extrapolation of higher strain rates

The extrapolation of the response for the higher strain rates is possible using the relationship proposed by Nagy et Al. [15]

$$\sigma(\varepsilon) = \sigma_0(\varepsilon) \times \left(\frac{\dot{\varepsilon}}{\dot{\varepsilon}_0} \right)^{n(\varepsilon)}$$

EQUATION 1 NAGY'S EXPRESSION FOR STRAIN RATE DEPENDENCE

$$n = n(\varepsilon) = a + b \times \varepsilon$$

EQUATION 2 EXPONENT FOR EQ. 3

In the expression the exponent *n* is a linear function of the strain, from that it is possible to write

$$\log\sigma(\varepsilon) - \log\sigma_0(\varepsilon) = n(\varepsilon) \times \left[\log\left(\dot{\varepsilon}\right) - \log\left(\dot{\varepsilon}_0\right)\right]$$

EQUATION 3 EXPERIMENTAL REGRESSION FOR N

And proceed with a linear fit in the plane $\log(\sigma) - \log(\dot{\varepsilon})$

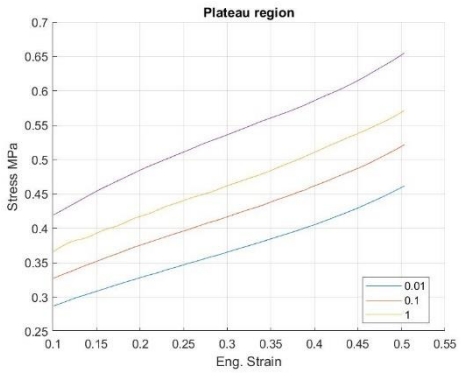

FIGURE 9 PLATEU REGION OF EXPERIMENTAL STRESS-STRAIN CURVES

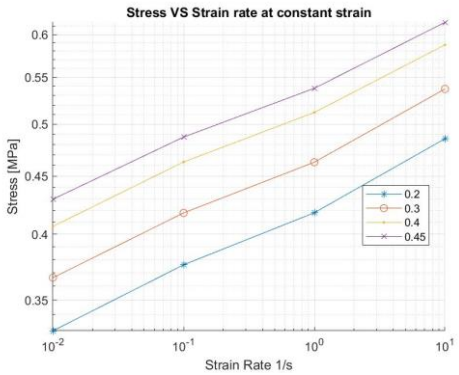

FIGURE 10 STRAIN RATE EFFECT

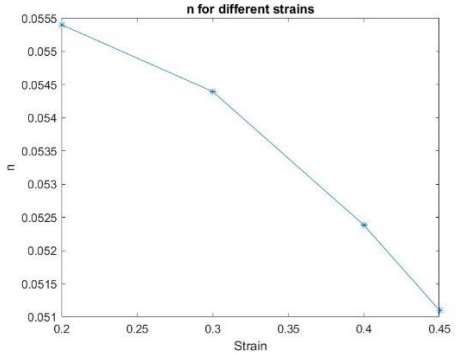

FIGURE 11 VALUES FOR N FOR DIFFERENT STRAINS

From this the coefficients *a* and *b* are obtained for EPP:

a= 0.0591

b=-0.0172

With a Matlab® script it is possible to generate the load curves for higher strain rates. To validate the method the extrapolated and the experimental curve for strain rate 10 s^{-1} are compared, as seen in the picture below, with good correspondence.

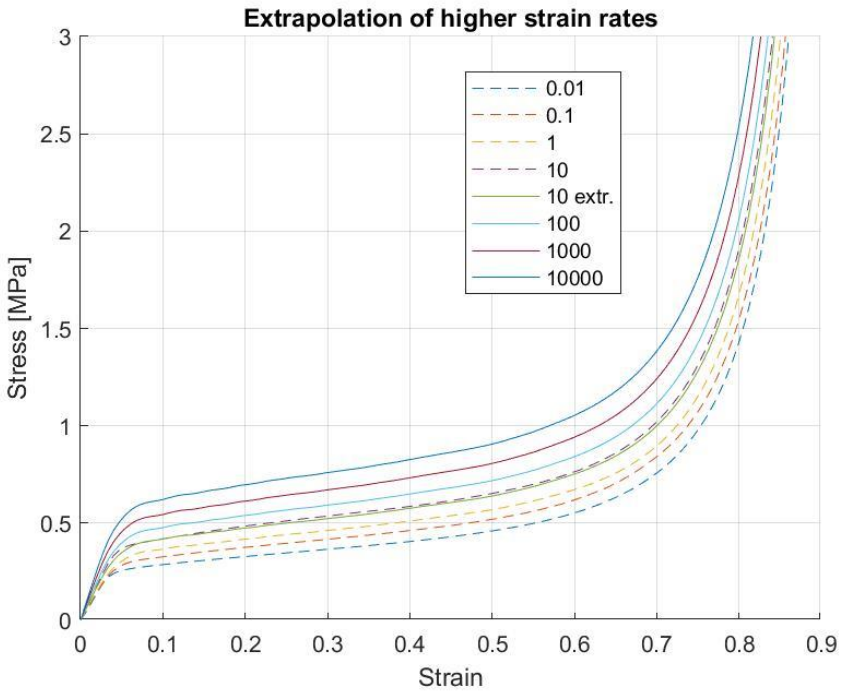

FIGURE 12 EXTRAPOLATED CURVES FOR HIGHER STRAIN RATES

The load curves have been resampled with 150 sampling points to facilitate the *table lookup* operation during the solution in LS-Dyna®.

The authors claim the method to be reliable for strain rate up to 100 s^{-1}, however, further studies carried out at KTH laboratories shows a good correspondence for higher strain rates.

Shear Test

Shear- compression combination is the most relevant loading that occurs in the helmet liner under oblique impact [16], as it can be seen in the picture below, representing the deformed zone of the frontal foam in a pitched impact. The shear properties of the liner, together with the friction at the head-liner and shell-impactor interface can be correlated with the rotational dynamic outcome of an oblique impact. It is therefore needed a good characterization of the shear response of the EPP material.

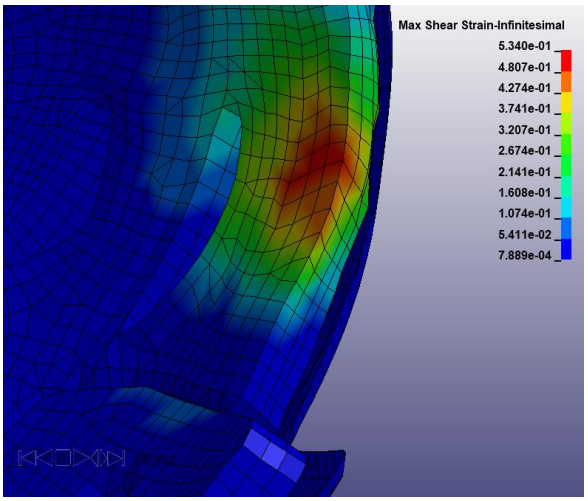

FIGURE 13 SHEAR DEFORMATION IN THE FRONTAL REGION

Several test procedures have been developed, some of these are based on a bi-axial test approach, as the one proposed by VandenBosche in [16]. Others proposed a simple shear test, although it is difficult to obtain a simple shear or pure shear strain distribution in the specimen all along the test. In matter of standards the references are the ASTM C-273 and the ISO 1922.

Looking at the ASTM C273, apart from the specimen size, the requirement to have the loading line passing through the opposite corners of the specimen and the system of pins that allows movement about two axis, avoiding a normal stress state between the plates to take place are the ones that are retained more important.

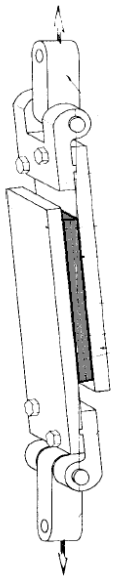

FIGURE 14 ASTM C273 SHEAR TEST RIG

Test setup

In the present work a test setup similar to the one prescribed in the ASTM C-273 is proposed as a balanced solution based on the needs of the KTH Neuronic Department.

The design aimed to generate a test rigging that fit the Instron® E3000 and allow the execution of tests on samples directly extracted from helmets in most of cases.

Due to limitations in the load and samples geometry a sample size of 75 mm x 15 mm x 20 mm is chosen and the specifications of new system defined.

The test rigging has been manufactured in the KTH Workshop in Flemingsberg by Peter Arfert, who developed the executive drawings that are reported in the appendix.

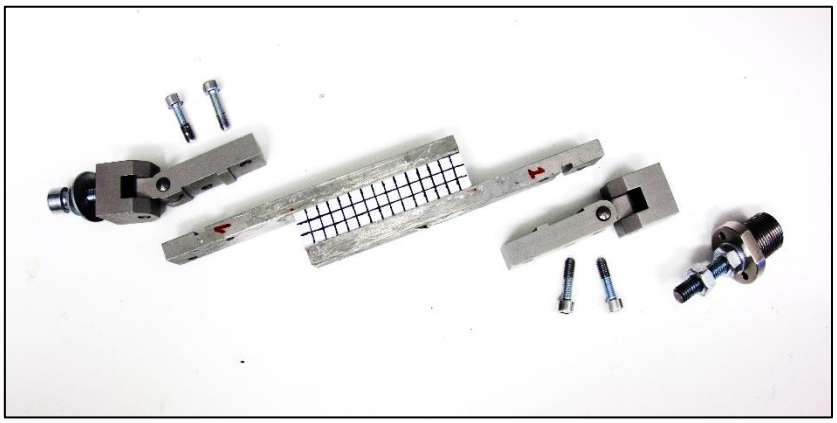

FIGURE 15 CUSTOM TEST RIG

The test rig is composed by a screw that fits the load cell, two ending part with unconstrained rotation about two axis, two interchangeable plates where the specimen is glued and that can be replaced during the test procedure to allow the execution of test on multiple samples.

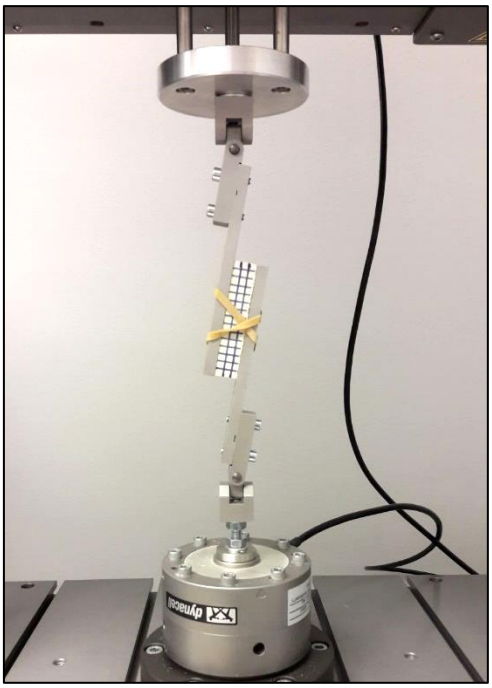

FIGURE 16 CUSTOM SHEAR TEST SETUP

The specimens are glued to the plates with an epoxy adhesive Araldite®2015 that performed well with EPP and other materials (*VERTEX SHOXS IV*), without dissolving the samples material or failing under test.

FIGURE 17 DEFORMATION OF THE SPECIMEN

The deformation can be evaluated by mean of motion tracking, making use of markers on the plates near the corners of the specimen. It was noted in the case of EPP testing that the length of the sides if an inner square of the grid remains almost constant (within 2%). The evaluation of the deformation by mean of a grid shows

that the sections remain almost flat except for the extremities where it is inevitable a complex stress-strain field. This results are confirmed by Finite Element simulation of the test.

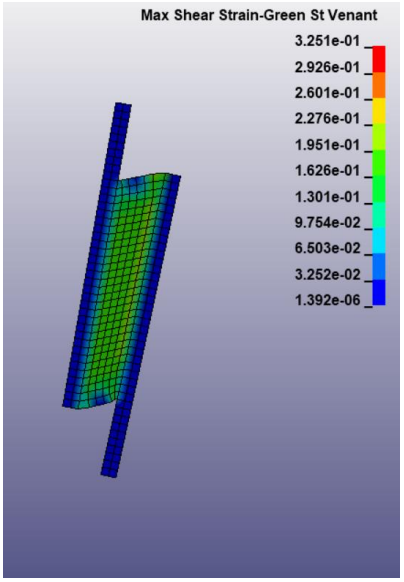

FIGURE 18 SHEAR STRAIN IN TEST SETUP FE SIMULATION

The tests have been conducted monitoring the shear stress and shear strain as they are defined in the ASTM-C273

$$\text{Shear stress: } \tau = \frac{F}{l \cdot w}$$

EQUATION 4 SHEAR STRESS FOR ASTM C273

$$\text{Shear strain: } \gamma = \frac{d}{h}$$

EQUATION 5 SHEAR STRAIN FOR ASTM C273

Where:

F= load [N]

D=displacement [mm]

L=specimen length (75mm)

W=specimen width (20mm)

H=specimen height (15mm)

The tested strain rates are 0.01 s^{-1}, 0.1 s^{-1}, 1 s^{-1}, 3 s^{-1}, 10 s^{-1}, however only the results of the first three are retained valid, as the test execution at 3 and 10 s^{-1} didn't show constant velocity during the ramp.

The tests have been performed in displacement control until the shear strain 0.5 corresponding to a displacement of 7.5mm. The direction of loading was the compressive one, with the extremities that moves close to each other.

Shear test results

The results show a noticeable dispersion, however due to the time required to clean and replace the samples with new ones a number of 3 or 4 has been considered acceptable.

There is a relevant hysteresis and the strain rate effect is relevant.

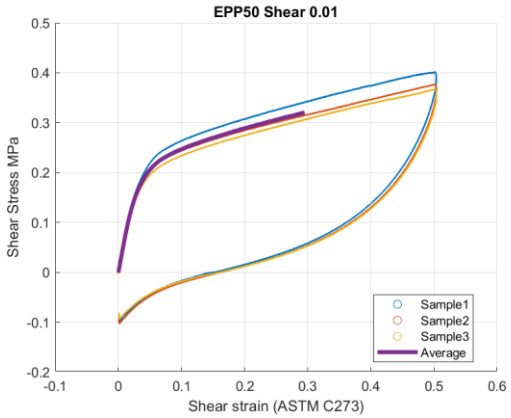

FIGURE 19 SHEAR STRESS STRAIN CURVES AT 0.15 MM/S

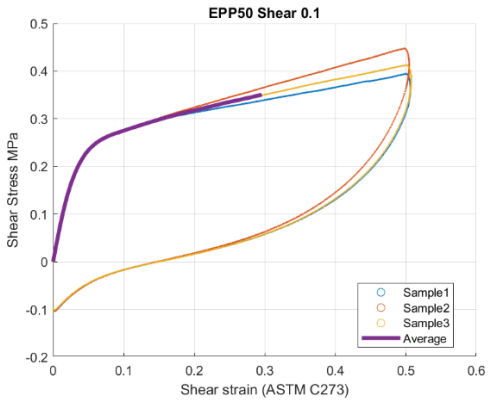

FIGURE 20 SHEAR STRESS STRAIN CURVES AT 1.5 MM/S

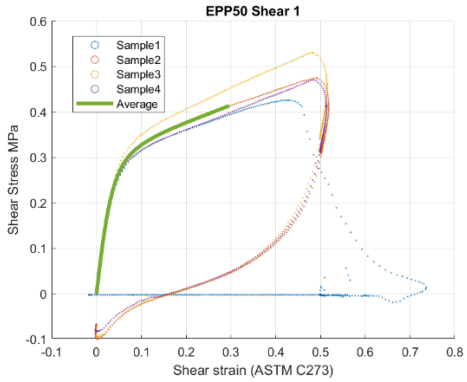

FIGURE 21 SHEAR STRESS STRAIN CURVES AT 15 MM/S

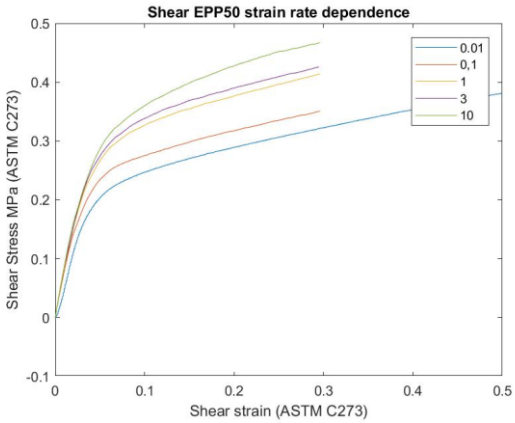

FIGURE 22 SHEAR STRESS-STRAIN CURVES FOR DIFFERENT STRAIN RATES

The experimental data have been treated in Matlab® 2018 where the curves have been averaged and prolonged until strain 1 to ensure stability in the case of direct implementation in LS-Dyna® material models.

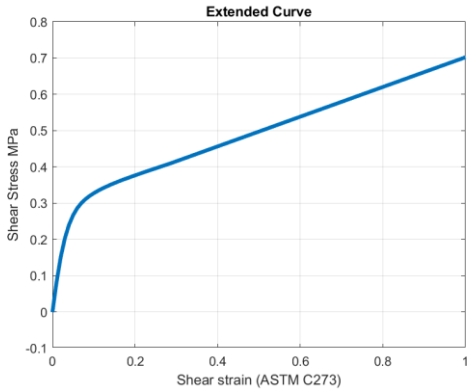

FIGURE 23 EXTENSION OF SHEAR STRESS-STRAIN CURVE FOR INPUT

Tensile Test

The tensile component is not expected to be dominant during head impact, but since many material models of LS-Dyna® require tensile curves as an input a test series is presented, and a series of curves generated.

Test setup

The setup is the same used in previous thesis work, the outcome of which has been published as open source FE model of helmet, except for the specimen size. It consist in a couple of T-shaped aluminum rigs on which the EPP specimens are glued.

With the possibility to test longer specimen the size has been modified from 20mm x 20mm x 20mm to 20 x 20 x 75 mm, to reduce the boundary effect during the tests. The glue used was the same of the shear tests and normally didn't show failure, although in many cases the specimen failure was located near the extremities.

FIGURE 24 TENSILE TEST SETUP

Tensile test results

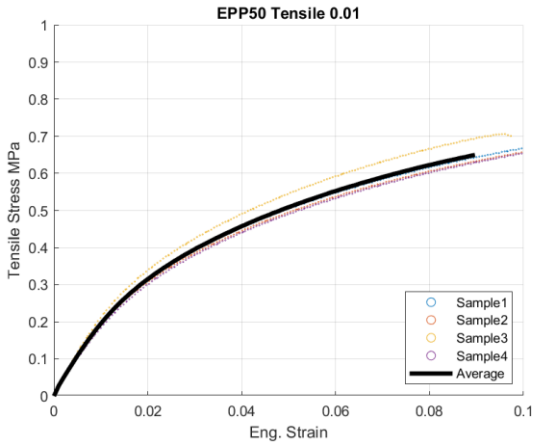

FIGURE 25TENSILE STRESS-STRAIN CURVES FOR STRAIN RATE 0.01 S-1

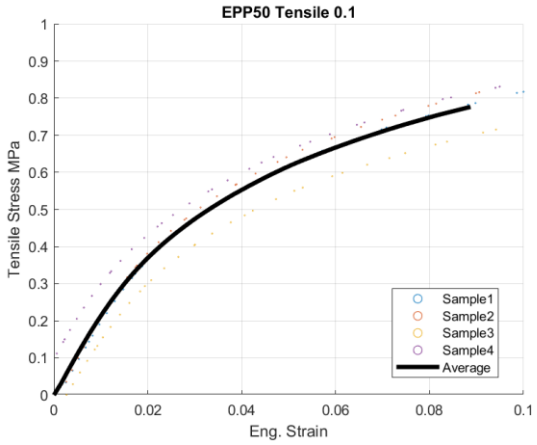

FIGURE 26 TENSILE STRESS-STRAIN CURVES FOR STRAIN RATE 0.1 S-1

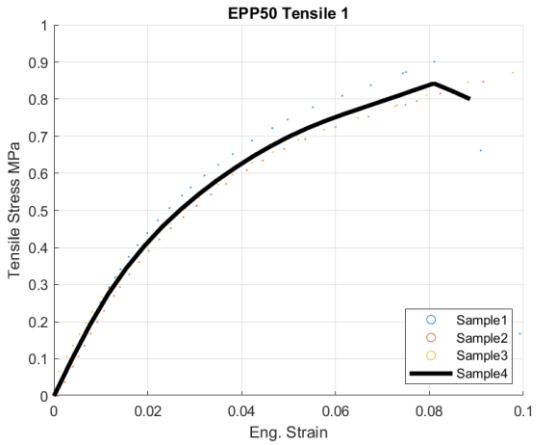

FIGURE 27 TENSILE STRESS-STRAIN CURVES FOR STRAIN RATE 1 S-1

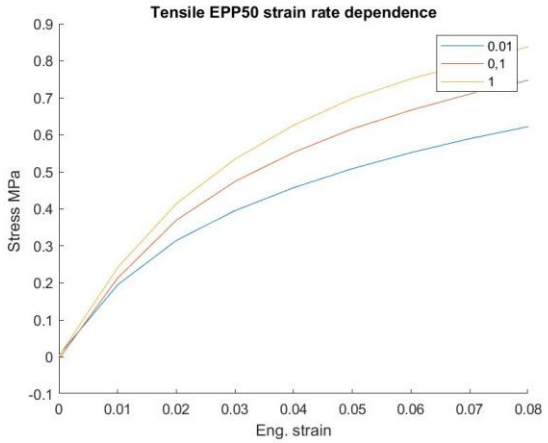

FIGURE 28 TENSILE STRESS-STRAIN CURVES FOR DIFFERENT STRAIN RATES

The tensile curves show a relevant strain rate effect.

The average curves for each strain rate have been processed with Matlab® and prolonged until 100% strain to be implemented in the desired material model. The slope of the added part was chosen to be the slope of the last experimental part, although this is not realistic for the tensile behavior it was helpful to match the shear response.

Material models in LS-Dyna®

The material models to simulate foamed materials that undergoes impacts are several, and of different grade of complexity. The ones more used in this type of simulation are:

*MAT_057_LOW_DENSITY_FOAM

Although this is not the natural material model to implement the EPP in a finite element analysis [17], MAT_057 is still one of the best candidates to simulate the EPP, one of its advantages is the possibility to insert an experimental stress-strain curve. It is possible to define a stiffness coefficient for contact interface stiffness (KCON), that allows to override the nominal elastic modulus in the contact computation, useful when two contacting parts are characterized by elastic properties that differ by order of magnitude, such in the case of the ABS shell and the EPP foam liner.

This material model allows to tune the unloading response by mean of the two factors *HU* and *SHAPE*, and to initialize the stress tensor in the foam using the *INITIAL_FOAM_REFERENCE_GEOMETRY card.

*MAT_063_CRUSHABLE_FOAM and *MAT_163_MODIFIED_CRUSHABLE_FOAM

These materials are dedicated to modeling crushable foams, with optional damping and tension cutoff. It is possible to assign a load curve defining stress versus volumetric strain. For the *163_MODIFIED_CRUSHABLE_FOAM it is possible to define a strain rate dependence by mean of a table of input curves corresponding to different deformation rates.

The fact that the EPP is not crushable (is recoverable) is in contrast with the specification of this material model, however it can be a candidate for a simple material model to be implemented as demontrated by the overall good response obtained in [1].

It is not possible to directly input a value for the elastic modulus, this cause the solver to compute the time step based on the density and maximum slope of the stress strain curve.

When the curve is defined with the procedure presented in the previous chapter, the higher strains part present a relatively high modulus compared to the low density of the expanded polymer, the time step is reduced unnecessarily causing the solution to run far longer than needed. One solution is to cut the input curve before it reach a too high slope, always considering the negative volume issues that can occur if the curve is truncated at a too small strain value.

*MAT_083_FU_CHANG_FOAM

This is the material that most authors suggest to implement EPP in LS-Dyna.

The formulation for this material include strain rate effect and allow the user to input the engineering stress strain data in the form of a table. The code interpolates between the available strain rates for the compressive-tensile loading. It's not

possible to directly assign a shear loading curve, but it is possible to achieve better shear response by mean of tuning the tensile part of the input curves.

It is possible to directly input a value for the elastic modulus to be used in the computation of the time step, so the complete compression curve can be given as input without an increase in the solution time.

By mean of the parameters *HU* and *SHAPE* it is possible to model the unloading response of the polymer.

It is possible to initialize the stress tensor in the material after performing a preliminary simulation where the foam is deformed.

*MAT_126_MODIFIED_HONEYCOMB

This material is intended to be used when simulating aluminum honeycomb plates, with anisotropic behavior. It is possible to assign load curves for both compression and shear loading.

Data preparation

The preparation of experimental data followed the sequence:

1. Data collection and import
2. Individuation of the beginning of displacements and cropping of the experimental curves to isolate the loading phase
3. Re-sampling and averaging of curve
4. After the experimental data range: For tensile and shear the curves follow with the last measured slope (for stability reason). For compression the curves are prolonged with polynomial extrapolation (exp 3) and linear extrapolation with compression modulus of the matrix material (2 GPa for PP).

   For MAT_83
5. Combination of the tensile curves with the compressive part, the tensile part is represented by negative values of strain. The tensile part is tuned im Matlab® to better replicate the shear behavior of the EPP.

Chapter 2 Helmet FE model

In this chapter are reported the choices regarding the material model, contact definition and additional control parameters that are necessary to overcome the criticalities that the FE modeling of impact presents. To be specific having large deformation in soft materials, and a moltiplicity of contact involving surfaces of different stiffness frequently result in unacceptable results and in some cases to errors that preclude the solution to be completed.

The solving method is explicit integration in LS-Dyna® and the pre-processing is carried out in LS-PrePost®, both available from LSTC [18].

Geometry and Mesh

The geometry was provided by a CAD file of the Easton Synergy 380 helmet. The geometry was cleaned and simplified, then meshed in Hypermesh by Isotta Rigoni (2017). No modifications are introduced since the mesh was retained good in term of stability and computational cost.

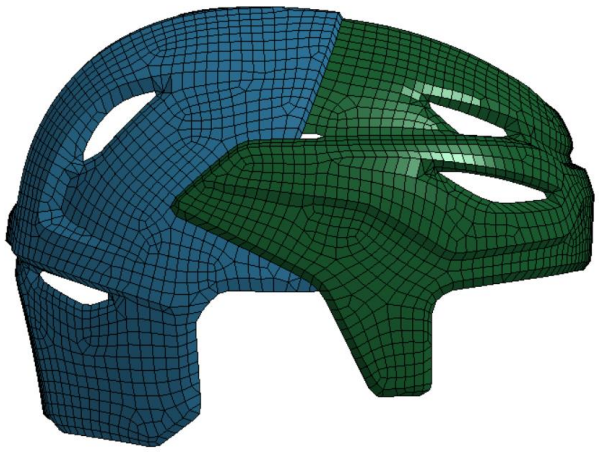

FIGURE 29 MESH OF THE HELMET'S SHELL (I. RIGONI, 2017)

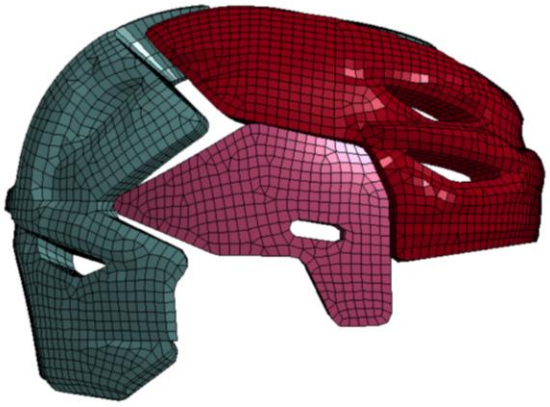

FIGURE 30 MESH OF THE HELMET EPP LINER (I. RIGONI, 2017)

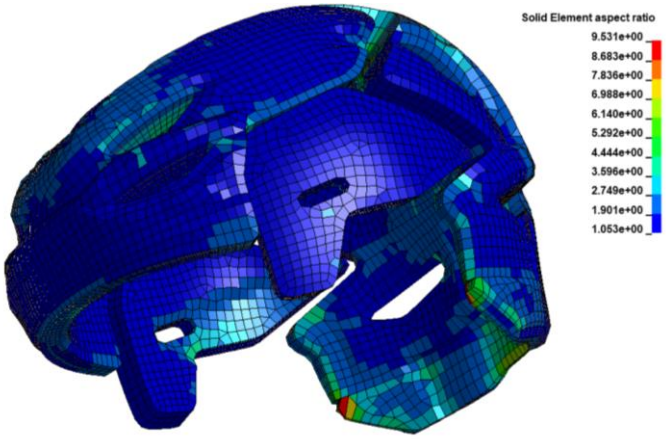

FIGURE 31ASPECT RATIO OF SOLID ELEMENTS IN THE EPP LINER

In total the helmet mesh is composed by:

- 66672 Shell elements (size approx. 5mm)
- 18486 Solid elements (size approx 5mm)
- 29928 Nodes

The finite element model with the included dummy head count 49010 nodes.

Element formulations

One frequently encountered problem was the occurrence of negative volume in the foam liner during the simulation. This is a frequent problem and can be

controlled by mean of the definition of an internal contact (*CONTACT_INTERIOR) on the parts that undergo large strains.

The element formulation plays an important role: using fully integrated element, or 20-nodes hexahedron, instead of 8-node constant stress element can easier result in one of the nodes passing through the opposite side and determine the calculation of a negative jacobian for the element, causing the simulation to stop.

For this reason, the foam is modeled with ELFORM=1 constant stress hexahedron elements, as suggested in [19].

The shells are modeled with the default ELFORM=2 Belitshko-Say

The dummy and impact surface are modeled with fully integrated solid elements and not modified.

Materials

The materials used for the helmet modeling are the ABS for the shell and the EPP foam for the liner.

ABS

The ABS is modeled in LS-PrePost with the card *MAT_001_ELASTIC

TABLE 3 INPUT PROPERTIES FOR ABS IN LS PRE-POST (*MAT_ELASTIC CARD)

RO Density	**E Young Modulus**	**PR Poisson Ratio**	**DA Additional parameter A**	**DB Additional parameter B**
1390	1.867e+09	0.25	0.0 (default)	0.0 (default)
Kg/m^3	Pa			

EPP

The definition of the EPP material model is reported for *MAT_083_FU_CHANG_FOAM_LOG_LOG_INTERPOLATION as in the validation process. The alternative solutions for the material model of the EPP comprises simpler material models in which the tensile curves input is excluded.

The LOG_LOG option is suggested where the input table is given in reason of logarithmic scaled abscissa values, such as 0.01 0.1 1, rather than linearly spaced values such 1,2,3 etc.

The input curves are the ones described before and the overall representation of the table is in the figure below. The curves are prolonged for stability reason until strain 1. The negative part of the curves correspon to the tensile input curves.

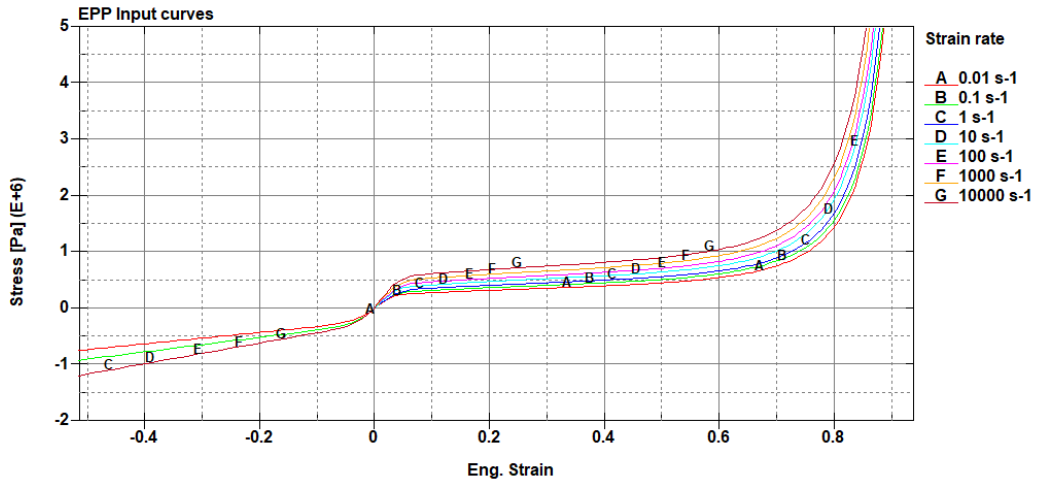

FIGURE 32 INPUT CURVES FOR EPP IN *MAT_083 FU CHANG FOAM

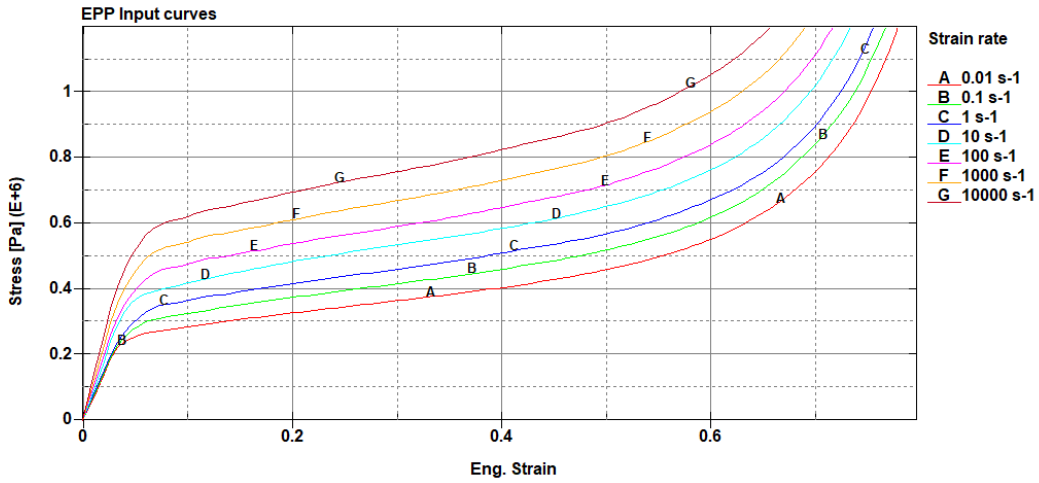

FIGURE 33 COMPRESSION PART OF THE INPUT CURVES FOR EPP 50

The additional coefficients defined are:

Young Modulus: E=7000000 Pa (7MPa)

Hystheretic Unloading factor: HU=0.2 (Default=1.0, i.e. no energy dissipation)

SHAPE=5 (Shape factor for unloading, values less than one reduces energy dissipation, greater than one increases dissipation)

As suggested from previous studies carried out on helmet's FE modeling.

DAMP=0.06 (Viscous coefficient to model damping effects)

Tensile Stress CutOff=1000000 Pa (1 MPa)

Where possible (*MAT057), the KCON option was set to 2*10^7 (Pa), that is about 1% of the elastic modulus of the ABS. This to avoid an excessive difference in the stiffness between the two contacting parts (foam and ABS shell) that may cause instability [20]. KCON overwrite the Young modulus of the material in the computation if contact force, it is useful when parts with large differences in the elastic modulus are put in contact.

For *MAT_057 , some modifications are made.

The compression input curve is the one that refer to the strain rate 100 s^{-1}.

In order to reduce the solution time a modification is apported because the high strain part of the compression curve is very steep, and in LS-Dyna the time-step is

computed referring to the highest value between the Young modulus of the material and maximum slope of the stress strain curves. For materials that base the calculation of the time step on the maximum slope of the stress strain curves a lower modulus (0.2 GPa) in the compacting section is chosen in order to have acceptable solution times. The curves remain the same until the beginning of the densification region at about.

Material model tuning and validation for MAT_083

To check the correspondence between experimental and simulated material properties a brief validation procedure was followed to ensure a good response in terms of stress-strain and in terms of strain rate dependence.

The material response was checked in compression, tension and shear by mean of single element simulation that replicate the experiments.

The tensile response was initially checked, but sacrificed in reason of the shear response, by tuning the tensile input curves ordinate and abscissa scaling factor (1.2 and 0.5 respectively), a better shear response in the plateau region was obtained. The tuned material is not expected to behave realistically in tension sinche the approach was to obtain a realistic compression-shear response, result achieved in the measure showed in the Figure 34 and Figure 35.

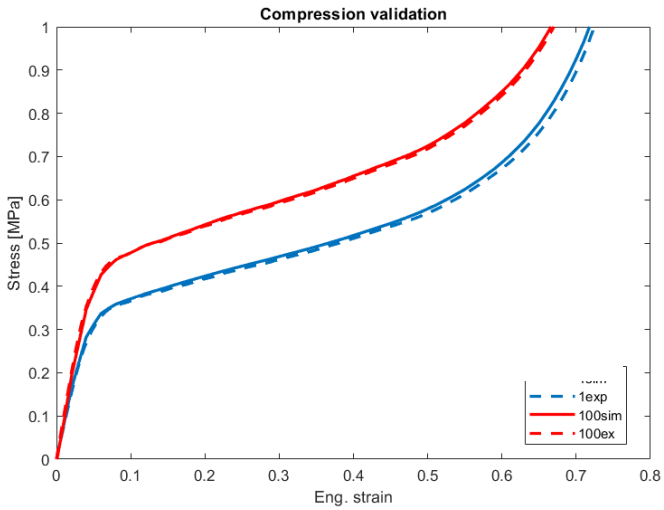

FIGURE 34 VALIDATION IN COMPRESSION

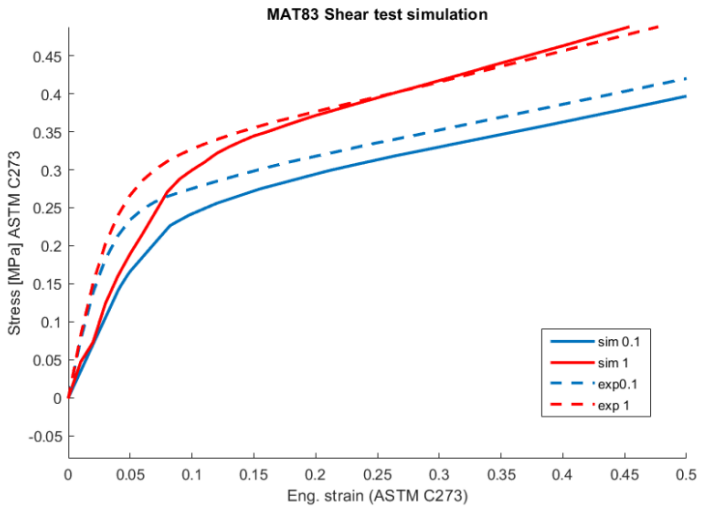

FIGURE 35 VALIDATION IN SHEAR

The compression simulation give close results compared to the experimental ones. The shear response, tuned with the scaling of the tensile curves, shows that the FEM of the material is more compliant than the real one in the elastic part of the curve, instead the part corresponding to the plateau is rather close. The strain effect is taken into account in both cases with success.

A possible improvement in this part could be the use of software such as LS_Opt [18] in which dedicated functionalities are present for such scope, in combination with drop tests on foam, to obtain a better material characterization and validation against more impact-relevant experimental measures. However, the present approach is supported by literature data and previous experiences carried out by the KTH students and researchers and is retained valid.

Dummy head FE model

The FE model of the head form is provided, and no modifications are made.

The model includes:

- Skull and skull-cap
- Rubber skin
- Two ballasts inside the skull
- Accelerometer

- Base for HIII model

The materials for the dummy are given and not modified.

The Skull, Accelerometer, Ballasts and Base are modeled as *RIGID to reduce the computational time

The aluminum skull is defined as *PART_INERTIA with initial translational velocity 6.25 m/s or 6.31 m/s corresponding to the impact case as will be precised in Table 11 initial velocities.

Helmet Part and Inertia definition

The helmet FE model is constituted by:

- The two parts of the ABS shell, that are then grouped into a *SET_PART
- The Lateral, Frontal and Posterior portion of the EPP liner, that are then grouped as a *SET_PART
- A shell of very thickness that overlap the foam, to help a correct behavior of the contact, modeled with elastic material with the characteristics of EPP.

Contacts Definition

The defined contacts are of different types. The parameters used ae reported, for more information the reader can refer to the LS-Dyna Keyword manual [21]

A shell of very small thickness was defined on the foam solid mesh, sharing the nodes with its surface. Then the contact between the dummy head and foam, and between foam and ABS shell is defined with this null shell.

Contact between Impact surface and Helmet shell: Is defined as AUTOMATIC_SURFACE_TO_SURFACE, between the *SET_PART including the two halves of the shell and the *PART identifying the oblique rigid surface. Friction coefficients is set to 0.7 as suggested by MIPS researchers, to simulate the friction between the ABS shell and the sandpaper sheet that lies on the oblique anvil surface. Other authors suggests 0.3 as friction coefficient value for the same purpose [22].

The contact between the dummy head and foam liner is defined as AUTOMATIC_SURFACE_TO_SURFACE with a friction coefficient of 0.5. MIPS engineers suggest values of 0.5 as standard rubber-to-EPP value, and values of 0.15 to simulate an additional low friction layer between head and helmet liner. Previous studies confirm this value to be reasonable, and tests performed in this case showed small dependence on the overall behavior during the impact. Other authors suggests 0.2 as EPS-HIII dummy friction coefficient [22], with good result in the simulation of bicycle helmet oblique impact. A dedicated study published in June 2018 [23] found that the EPS – HIII friction coefficient is about 0.75.

The constraint between helmet shell and foam liner is defined as TIED_SHELL_TO_SURFACE. Attention must be put to reduce unwanted penetration, evaluating the relative thickness of the two contacting shells and scaling them properly. Not all the nodes of the shell and foam surface are tied, but only the ones where the two parts are closer, this condition is supposed to replicate the behavior of the physical model where gaps are present as visible from the CAD file of the Easton Sinergy 380. The SOFT=1 option, with SFSCL=0.1 was effective to manage the contact between the foam and the helmet shell without the occurrence of unwanted penetration.

The different way of defining which nodes of the contacting shells are tied, should replicate the real characteristic of the shell to foam bonding in the helmet.

A CONTACT_AUTOMATIC_SURFACE_TO_SURFACE is defined between the foam shell and the helmet shell, with SOFT=1, SFSCL=0.1.

TABLE 4 DUMMY TO EPP FOAM CONTACT PARAMETERS

Dummy head to Helmet									
*CONTACT_AUTOMATIC_SURFACE_TO_SURFACE									
Slave	Master	FS	FS	SFS	SFM	SFST	SFMT	SOFT	SOFSCL
Foam null Shell (Part)	Dummy (Part)	0.5	0.5	0	0.25	1	1	2	0.1
SNLOG	VDC								
1	10								

TABLE 5 EPP FOAM TO SHELL CONTACT PARAMETERS

Helmet Shell to Foam									
*CONTACT_AUTOMATIC_SURFACE_TO_SURFACE									
Slave	Master	FS	FS	SFS	SFM	SFST	SFMT	SOFT	SOFSCL
Foam (Part)	Helmet shell (Part)	0.5	0.5	1	1	1	1	1	0.1

TABLE 6 TIED CONTACT FOAM TO SHELL PARAMETERS

Helmet Shell to Foam									
*CONTACT_TIED_SURFACE_TO_SURFACE_OFFSET									
Slave	Master	FS	FS	SFS	SFM	SFST	SFMT	SOFT	SOFSCL
Foam (Part)	Helmet shell (Part)	0.1	0.1	10	1	1	10	1	0.1

TABLE 7 FOAM-TO-FOAM CONTACT PARAMETERS

Contact between foam liner parts									
*CONTACT_AUTOMATIC_SURFACE_TO_SURFACE									
Slave	Master	FS	FS	SFS	SFM	SFST	SFMT	SOFT	SOFSCL
Foam A	Foam B	0.5	0.5	10	10	1	1		

TABLE 8 INTERIOR CONTACT FOR THE EPP FOAM PARAMETERS

Contact INTERIOR foam liner	
*CONTACT_INTERIOR	
Part set id	Foam

TABLE 9 CONTACT BETWEEN ALUMINUM SKULL AND DUMMY SKIN PARAMETERS

Dummy skin to Skull									
*CONTACT_AUTOMATIC_SURFACE_TO_SURFACE									
Slave	Master	FS	FS	SFS	SFM	SFST	SFMT	SOFT	SOFSCL
Foam (Part)	Helmet shell (Part)	0.8	0.8	1	1	1	1	2	0.1

TABLE 10 CONTACT BETWEEN HELMET SHELL AND IMPACT SURFACE PARAMETERS

Helmet Shell to Impact Surface									
*CONTACT_AUTOMATIC_SURFACE_TO_SURFACE									
Slave	Master	FS	FS	SFS	SFM	SFST	SFMT	SOFT	SOFSCL
Helmet Shell (P. set)	Impact Surface (Part)	0.7	0.7	1	1	1	1	1	0.1

Chapter 3 Finite Element Model simulations

In this chapter a description of the main characteristics of the simulation is proposed. The simulation performed were of two type: fitting of the helmet on the dummy head and impact simulation. The helmet size used in the drop test is M.

Fitting of head form

A suggested procedure used in other cases was to fit the head form inside the helmet prior to perform impact simulations.

The FEM helmet dimensions were checked and the helmet was re-scaled at the original dimensions since the original model ("not fitted") included a version of the helmed scaled out for 2% and 3% in longitudinal and transverse direction.

This can overcome the issue of dealing with initial penetration that occurs inevitably when positioning the head form in the helmet and is supposed to provide a replication of the actual fitting achieved in the experimental phase. An evaluation of the effect is presented for one of the test case.

The simulation takes long time (25 hrs. on the KTH Cluster) because long termination time was needed to let the oscillations amplitude to become small enough and the position of the node to be stable.

The fitting is performed by mean of:

1. Manual positioning of the head/helmet. No references were available, so a reasonable positioning was assumed, with a very small overlapping of the head / helmet volumes.
2. Scaling the head form to 90% of the initial dimensions
   Only the skin of the dummy is considered for this operation, then the remaining components are reintroduced for the impact simulations.
3. Simulation of the head form that return to its full dimensions contacting the foam liner with the *PRESCRIBED_FINAL_GEOMETRY card (Figure 36).

The curve governing the process must be shaped to ensure a slow initial contact between the parts, to reduce the oscillations that normally will occur.

4. Verification of pressures and deformation to ensure that no unreasonable values are present.
5. Exporting the fitted position of nodes of the Head/Helmet to be used in the definition of the parts.

FIGURE 36 FITTING PROCEDURE OF THE HELMET

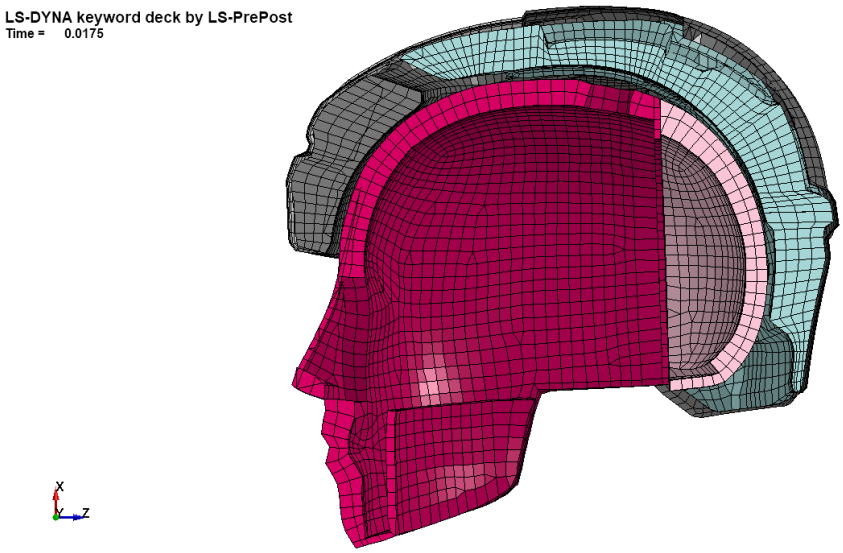

FIGURE 37 NOT FITTED HEAD/HELMET SECTION

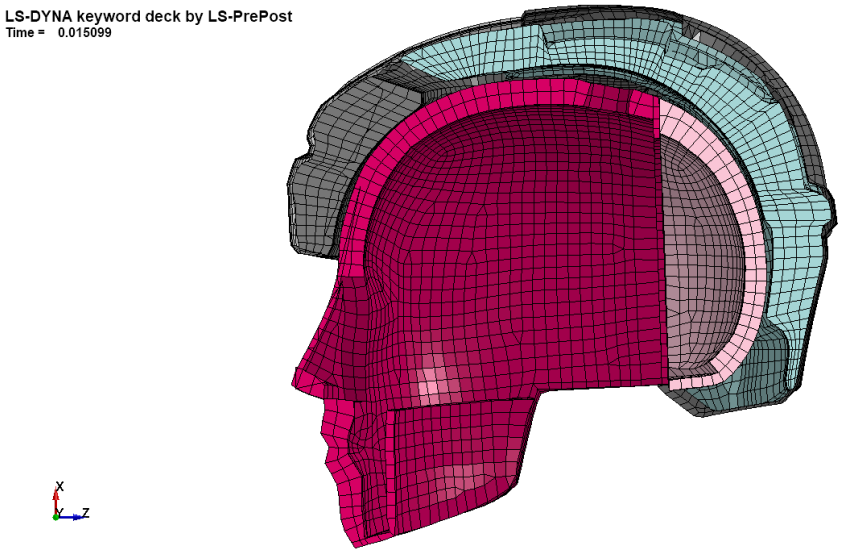

FIGURE 38 FITTED HEAD/HELMET SECTION

An advantage of the *MAT_83 over the others is the possibility to initialize the stresses in the foam by mean of the undeformed foam nodes coordinates input using the *INITIAL_FOAM_REFERENCE_GEOMETRY card. [1]

Impact Simulations

The simulations performed aimed to represent an oblique impact under three different configurations, all the three involving oblique impact.

The internal codes used at MIPS for the archiviation of the tests are 7538 (Backward), 7491 (Lateral), 7493 (Pitched).

The execution was performed on an oblique impact drop test rig similar to the one present at the KTH Neuronic department and represented in Figure 4.

The velocities prior to impact, from nominal height 2.2m, and the configuration are illustrated in Figure 39.

[1] The solution of the model with the initialized stress was not possible at present because of signaled license errors when prompted. The effect of the geometrical fitting is considered without the initial stress that probably affect the behavior of the system.

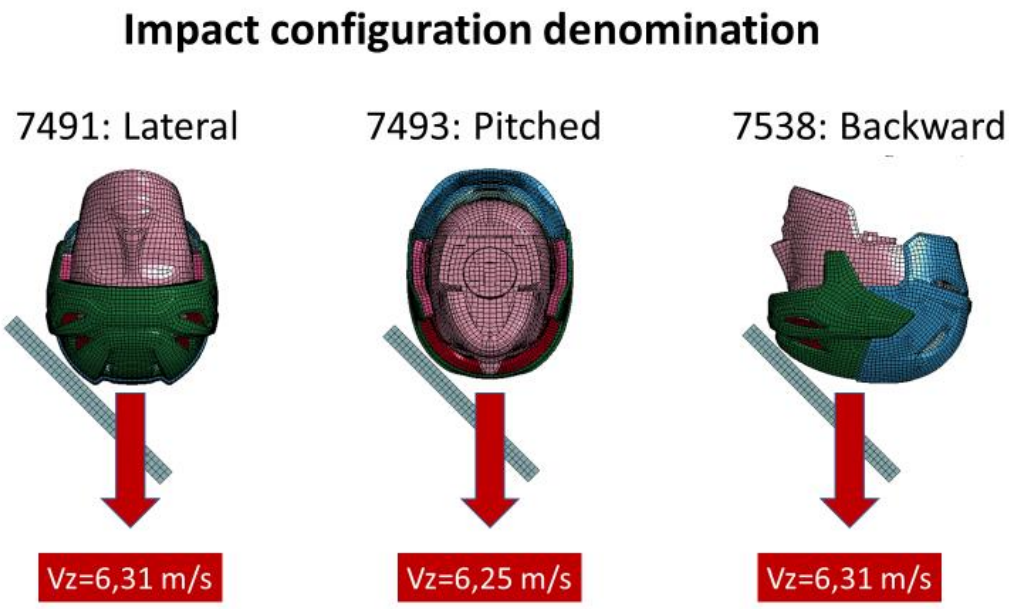

FIGURE 39 CORRESPONDENCE TEST CODE AND IMPACT CONFIGURATION

TABLE 11 INITIAL VELOCITIES

Initial velocity		
7491 (Lateral)	7493 (Pitched)	7493 (Backward)
6.31 m/s	6.25 m/s	6.31 m/s

The kinematic parameters are evaluated with reference to the node corresponding to C.O.M of the head form. (Node 50115516).

Several material models are tested, although more effort has been put in the definition of the *MAT_057_LOW_DENSITY_FOAM and *MAT_083_FU_CHANG_FOAM as the suggested one from the literature [17]. Also *MAT_063 and *MAT_163 (Crushable and Modified Crushable Foam) were considered as options, but the discarded because of the non recoverable behavior of these material models in contrast with the characteristics of EPP.

The procedure was that of incrementally add modifications to the existing model, once that the problems regarding the contacts were solved.

In the following several configuration are presented changing the material formulation and including or not the fitting of the helmet. In the FIT cases the helmet was fitted following the procedure previously described. In the NOT FIT cases the helmet is kept with a 2% scaling in order to be positioned without the occurrence of initial penetration between head and helmet nodes.

TABLE 12 DETAILS OF THE TESTED CONFIGURATIONS

Tested configurations			
Conf. ID	Mat. Model	Mat. notes	Fitting
A1	083_Fu_CHANG_FOAM	Validated in shear with tuning of the tensile input curves	YES
A2	083_Fu_CHANG_FOAM	Validated in shear with tuning of the tensile input curves	NO
A3	083_Fu_CHANG_FOAM	linear elastic tensile response with cut-off at 0.1 MPa	NO
B1	057_LOW_DENSITY_FOAM	Compression curve at strain rate 100 s^{-1}	YES
B2	057_LOW_DENSITY-FOAM	Compression curve at strain rate 100 s^{-1}	NO

General Settings

TABLE 13 CONTROL SETTINGS FOR IMPACT SIMULATIONS IN LS PREPOST

Control						
Termination time	0.02 (s)					
Energy	HGEN=2	RWEN=2	SLNTEN=2	RYLEN=2		
Timestep	TSSFAC=0.6					

TABLE 14 HOURGLASS SETTINGS IN LS PREPOST

Hourglass	
Type: 3	IHQ=0.15

TABLE 15 OUTPUT SETTING FOR IMPACT SIMULATIONS IN LS PREPOST

Database	
General Result write interval 0.0001 s	
ASCII_option	GLSTAT, MATSUM, NODOUT, SLEOUT
History_node	(Nodes of the Accelerometer, 50115516 is the c.o.m in this case)

General observations

The solution time changes between 40 min and 2h:30 min on a Intel i7 4720 (3ghz) processor.

Stability

The main concerns are related to contact instabilities and the occurrence of negative volume errors. Several attempts needed to be done to run the solution without errors.

The Pitched impact simulations were usually slower, during the solution the time step is reduced to the order of magnitude of 10^{-8} s, while for the other configurations it remain stable at values around $4*10^{-7}$s.

The hourglass energy was a few point percentage of the total energy.

Troubleshooting

The instability is mosltly determined by the huge difference in the elastic properties of contacting materials and by the large deformations that these undergo.

Regarding the contact issues the suggestion is to set the option SOFT=1, and to disable the shooting node logic with SNLOG=1. This feature is rpesent to avoid instability in the case a slave node is “found” well behing the master surface and a elevate contact force is applied instantly. The shooting node logic simply “replace” the node without applying any force, this can result in a bad element shaping ad drive to negative volume errors.

The other factor that may contibute are the reduction of the time step scale factor (in some case it was reduced to 0.5) and the use of interior contact on the foam part set.

Results

The results of the simulation are filtered with a SAE 300 filter directly in LS PrePost.

The value of 300 Hz is chosen to smooth the curves, although the standards for helmet testing requires usually a 1000 Hz or 600 Hz filtering this because the experimental data are available in the already filtered form and no information is provided about the filtering procedure used at the time. When necessary the curves are shifted in time in an attempt to mimic the actual triggering.

Configuration A1 *MAT_083 fitted, with tensile curves (validated material)

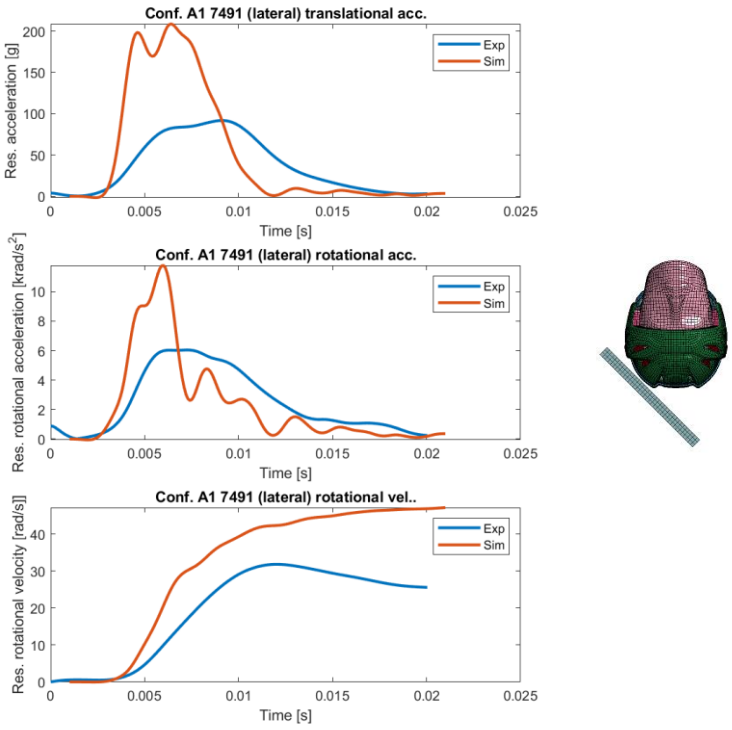

FIGURE 40 CONF. A1 LATERAL IMPACT

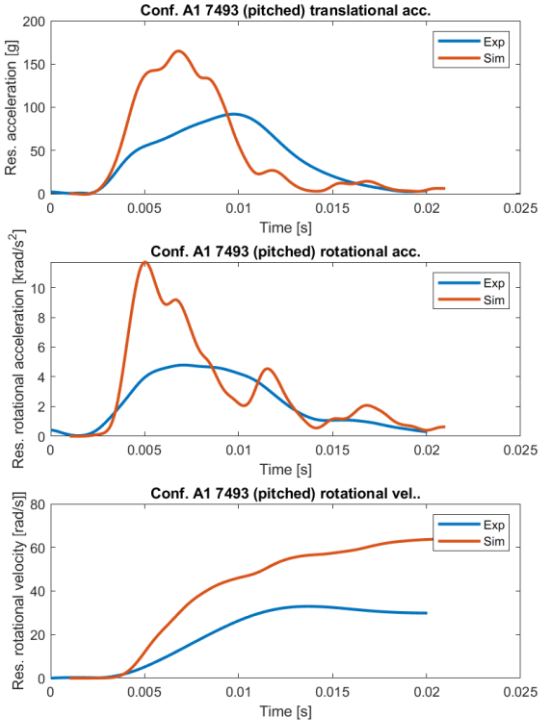

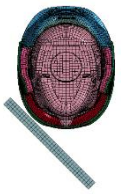

FIGURE 41 CONF. A1 PITCHED IMPACT

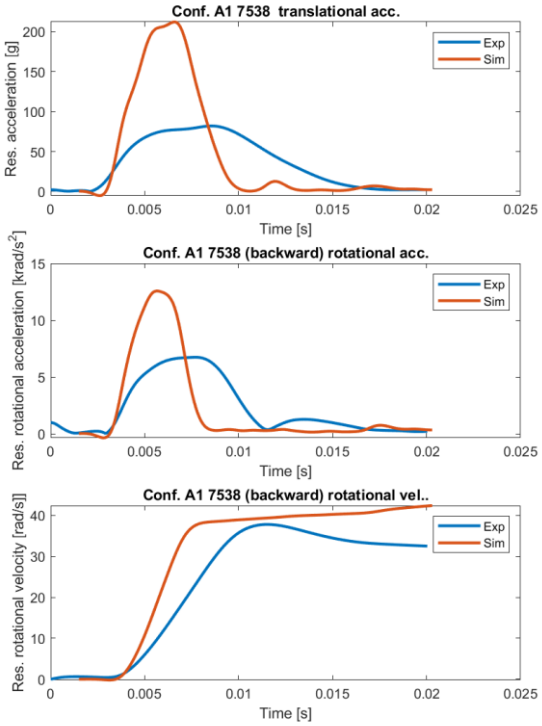

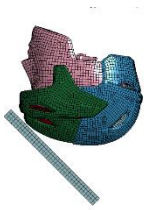

FIGURE 42 CONF. A1 BACKWARD IMPACT

Configuration A2 *MAT_083 Not Fitted (Validated material)

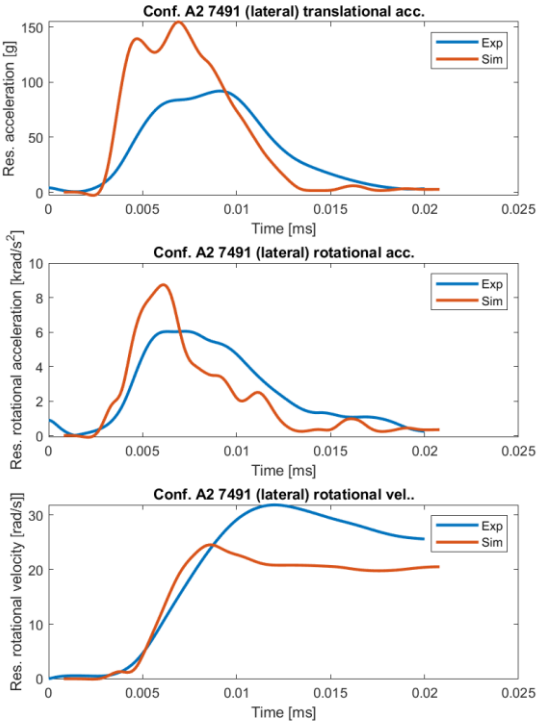

FIGURE 43 CONF. A2 LATERAL IMPACT

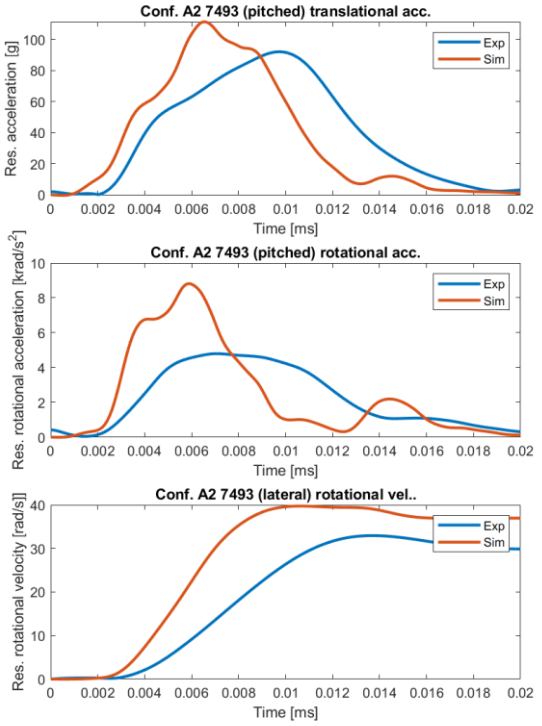

FIGURE 44 CONF. A2 PITCHED IMPACT

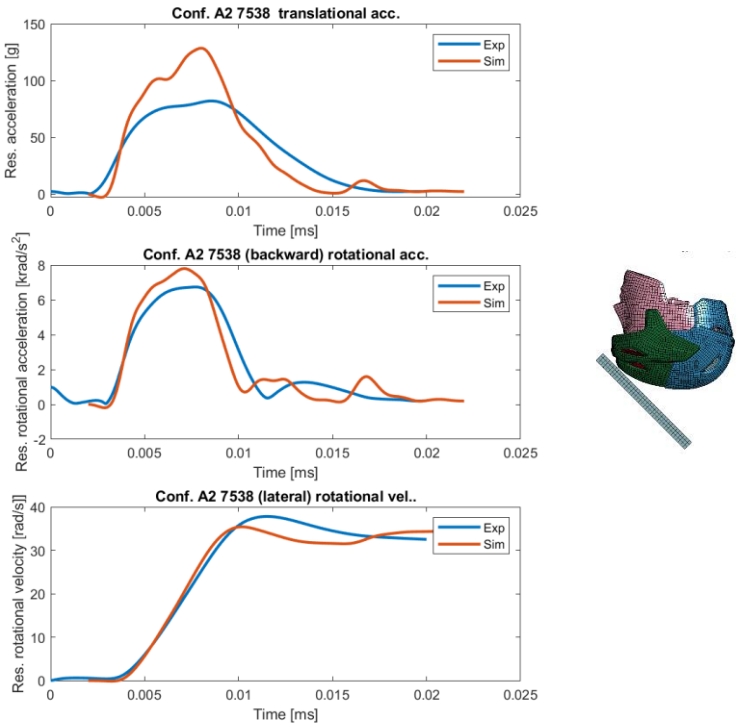

FIGURE 45 CONF. A2 BACKWARD IMPACT

Configuration A3*MAT_083_Not Fitted, linear tensile response

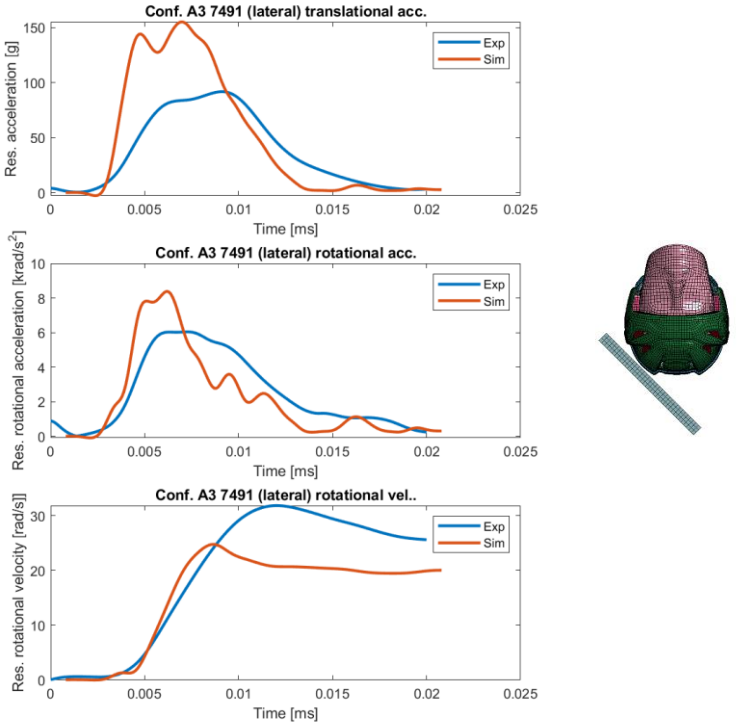

FIGURE 46 CONF. A3 LATERAL IMPACT

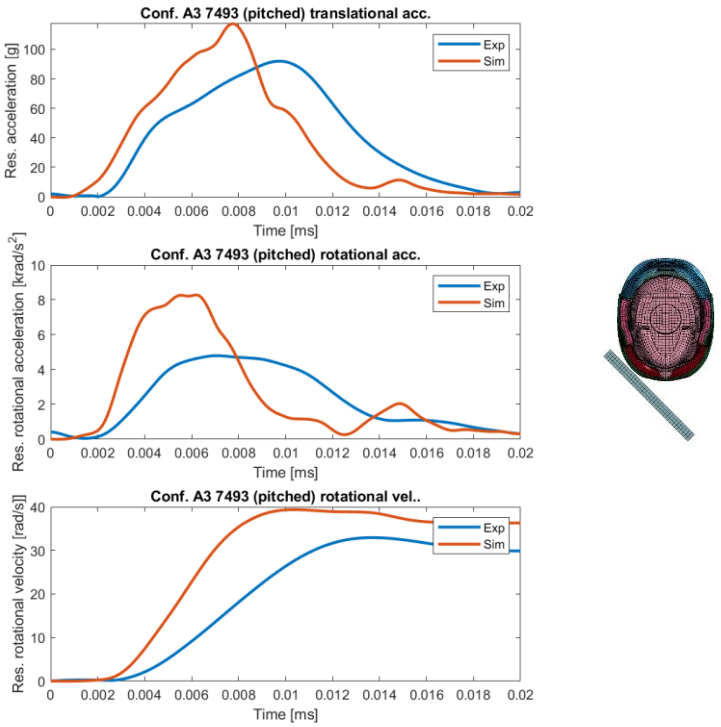

FIGURE 47 CONF. A3 PITCHED IMPACT

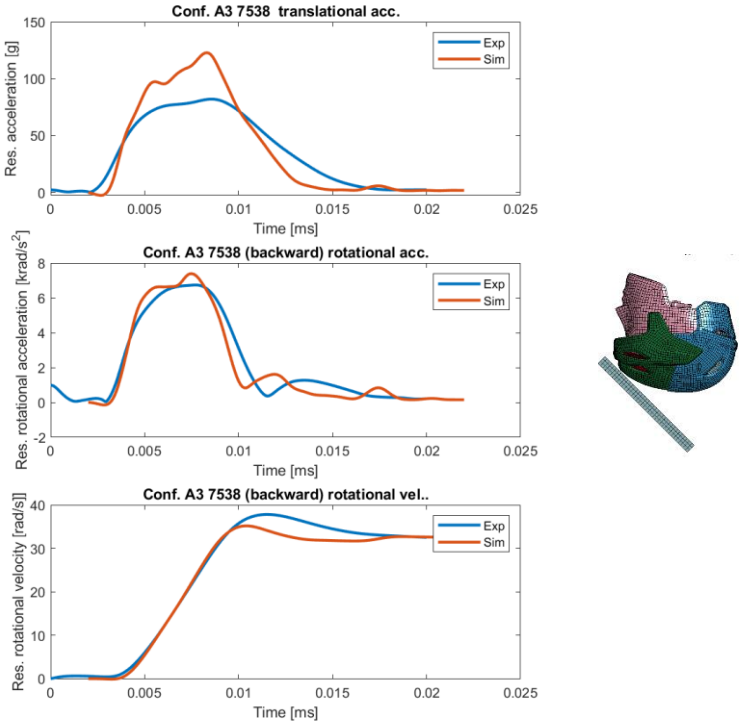

FIGURE 48 CONF. A3 BACKWARD IMPACT

Configuraton B1 *MAT_057 fitted

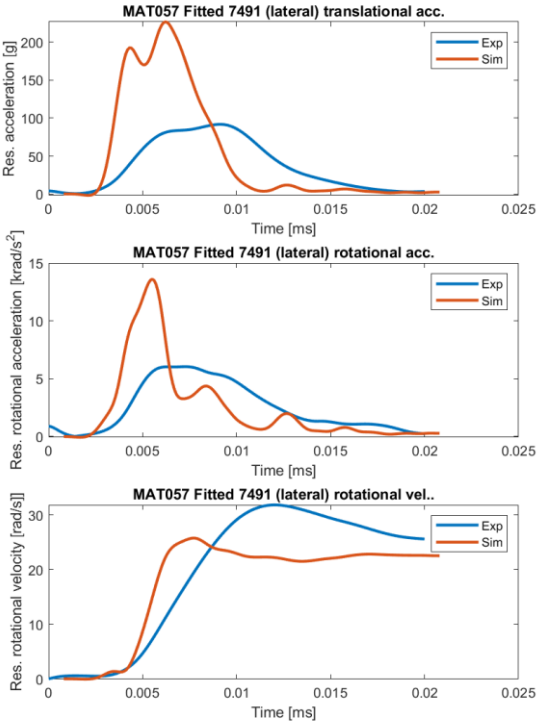

FIGURE 49 CONF. B1 LATERAL IMPACT

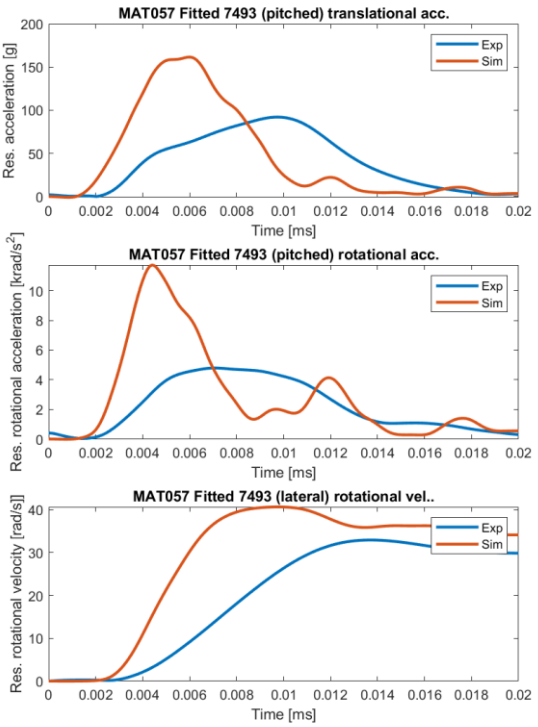

FIGURE 50 CONF. B1 PITCHED IMPACT

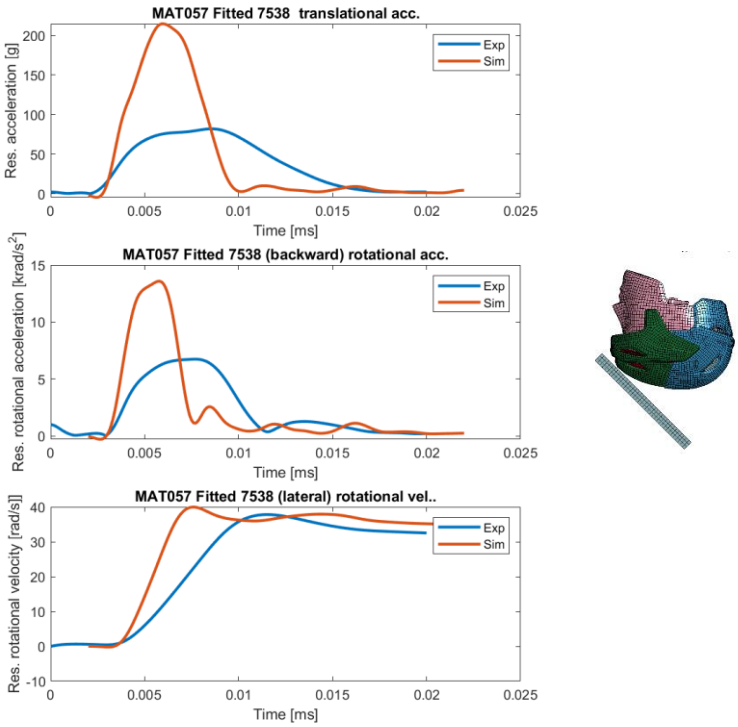

FIGURE 51 CONF. B1 BACKWARD IMPACT

Configuration B2*MAT_057 not fitted

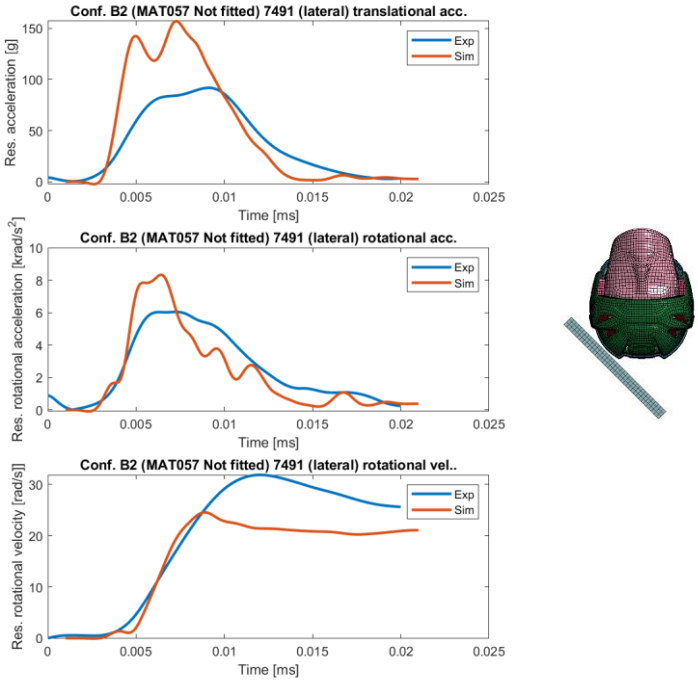

FIGURE 52 CONF. B2 LATERAL IMPACT

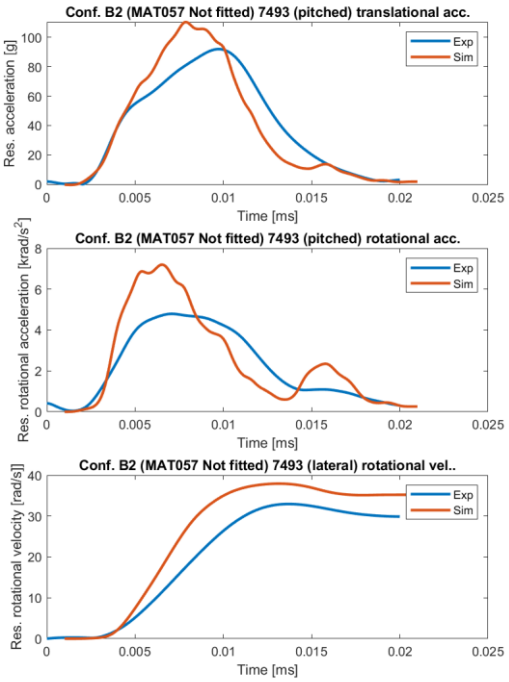

FIGURE 53 CONF B2 PITCHED IMPACT

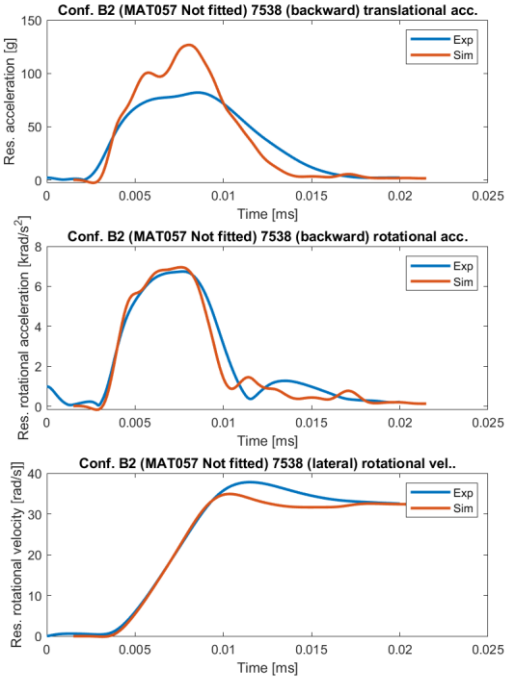

FIGURE 54 CONF. B2 BACKWARD IMPACT

Correlation analysis

The similarity between the experimental and simulated curves is measured by mean of the Pearson correlation coefficient r and r^2 [24]

$$r = \frac{\sum_{i=1}^{n}(x_i - \bar{x})(y_i - \bar{y})}{\sqrt{\sum_{i=1}^{n}(x_i - \bar{x})^2 \sum_{i=1}^{n}(y_i - \bar{y})^2}}$$

EQUATION 6 PEARSON'S CORRELATION COEFFICIENT

A1 configuration: correlation coefficients

TABLE 16 PEARSON CORRELATION COEFFICIENT, A1 CONFIGURATION

A1, r	**r , lateral**	**r pitched**	**r backward**
Tr. accel.	0,44	0,48	0,33
Rot. accel.	0,43	0,58	0,19
Rot. Vel	0,95	0,97	0,88

TABLE 17 R^2, A1 CONFIGURATION

A1, r^2	**r^2 lateral**	**r^2 pitched**	**r^2 backward**
Tr. accel.	0,19	0,23	0,11
Rot. accel.	0,18	0,34	0,04
Rot. Vel	0,91	0,94	0,77

A2 configuration: correlation coefficients

Conf. A2, r	**r , lateral**	**r pitched**	**r backward**
Tr. accel.	0,67	0,78	0,60
Rot. accel.	0,64	0,65	0,49
Rot. Vel	0,88	0,94	0,89

Conf. A2, r^2	r^2 lateral	r^2 pitched	r^2 backward
Tr. accel.	0,44	0,61	0,36
Rot. accel.	0,41	0,42	0,24
Rot. Vel	0,78	0,89	0,80

A3 configuration: correlation coefficients

TABLE 18 PEARSON CORRELATION COEFFICIENT, A3 CONFIGURATION

A3, r	r , lateral	r pitched	r backward
Tr. accel.	0,68	0,77	0,64
Rot. accel.	0,65	0,64	0,53
Rot. Vel	0,87	0,94	0,91

TABLE 19 R^2, A3 CONFIGURATION

A3, r^2	r^2 lateral	r^2 pitched	r^2 backward
Tr. accel.	0,46	0,60	0,42
Rot. accel.	0,42	0,41	0,28
Rot. Vel	0,76	0,88	0,82

B1 configuration: correlation coefficients

TABLE 20 PEARSON CORRELATION COEFICIENT, B1 CONFIGURATION

B1. r	r , lateral	r pitched	r backward
Ttr. accel.	0,39	0,49	0,20
Rot. accel.	0,35	0,52	-0,01
Rot. Vel	0,81	0,86	0,73

TABLE 21 R^2, B1 CONFIGURATION

B1, r^r	r^2 lateral	r^2 pitched	r^2 backward
Ttr. accel.	0,16	0,24	0,04
Rot. accel.	0,12	0,27	0,00
Rot. Vel	0,65	0,74	0,53

B2 Configuration: correlation coefficients

TABLE 22 PEARSON CORRELATION COEFFICIENT, B2 CONFIGURATION

B2, r	r , lateral	r pitched	r backward
Ttr. accel.	0,71	0,79	0,76
Rot. accel.	0,69	0,68	0,69
Rot. Vel	0,90	0,95	0,94

TABLE 23 R^2, B2 CONFIGURATION

B2, r^4	r^2 lateral	r^2 pitched	r^2 backward
Ttr. accel.	0,49	0,63	0,58
Rot. accel.	0,48	0,46	0,47
Rot. Vel	0,81	0,91	0,89

To have an overview of how each configuration correlate with the experimental results the average correlation coefficients for the three impact (lateral, pitched and backward) were calculated and are presented in Figure 55, Figure 56 and Figure 57.

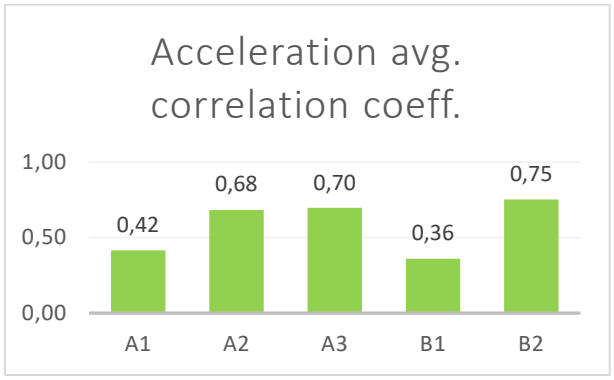

FIGURE 55 AVERAGE CORRELATION COEFFICIENTS FOR LINEAR ACCELERATION

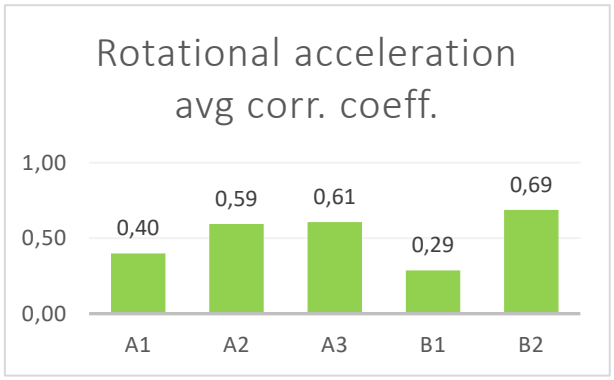

FIGURE 56 AVERAGE CORRELATION COEFFICIENTS FOR ROTATIONAL ACCELERATION

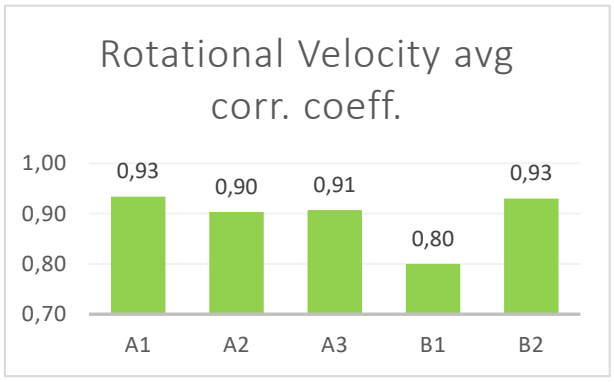

FIGURE 57 AVERAGE CORRELATION COEFFICIENTS FOR ROTATIONAL VELOCITY

Peak linear acceleration score

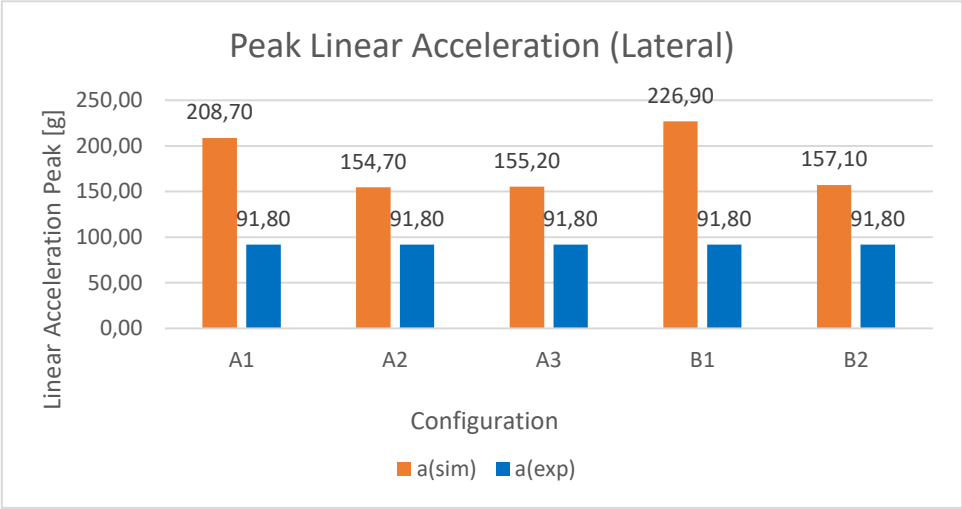

FIGURE 58 LINEAR ACCELERATION PEAK VALUES, LATERAL

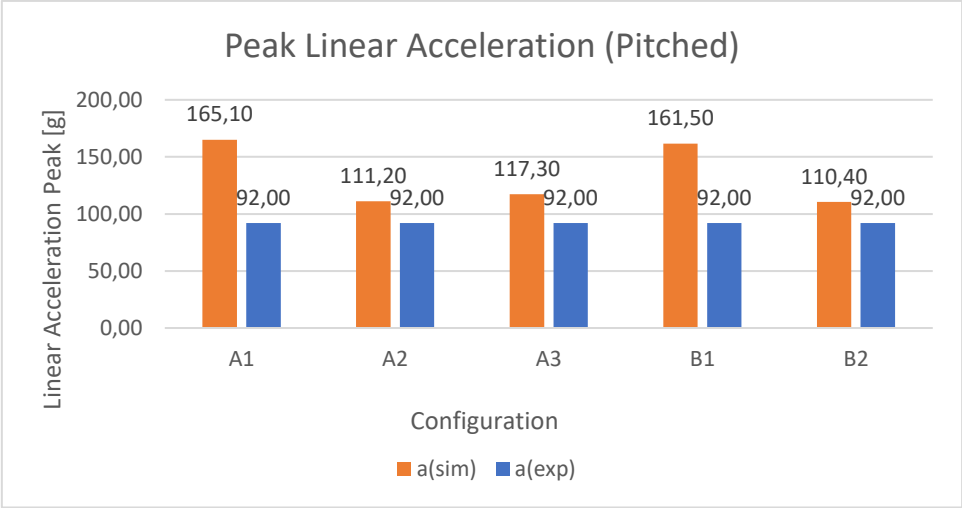

FIGURE 59 PEAK LINEAR ACCELERATIONS, PITCHED

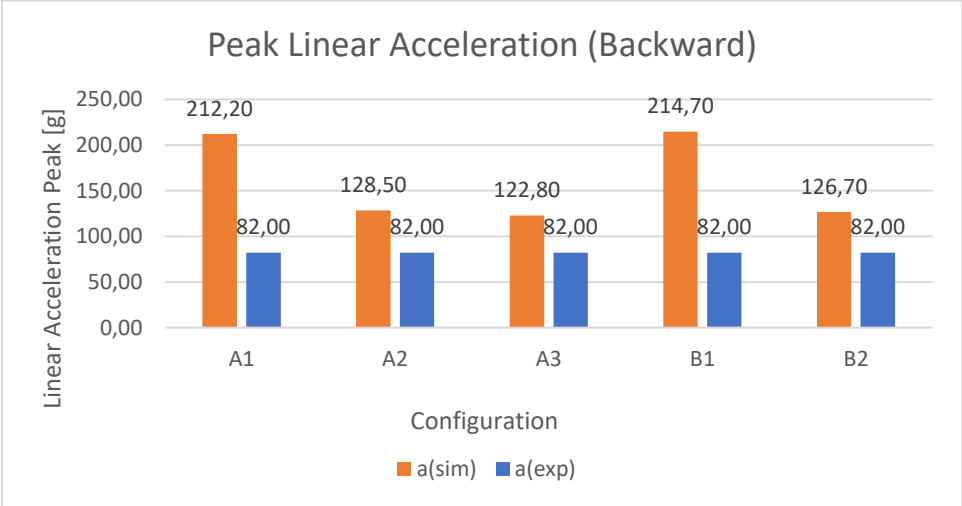

FIGURE 60 PEAK LINEAR ACCELERATIONS, BACKWARD

The Peak linear acceleration Score (PS) correlate simulated and experimental values of the linear acceleration by mean of the index PS. Value higher than 80 are considered acceptable.

$$\mathrm{PS}\ (\%) = \left[1 - \left[\frac{|a_{sim} - a_{exp}|}{a_{exp}}\right]\right] \times 100$$

EQUATION 7 PEAK LINEAR ACCELERATION SCORE

.

The values for the peak linear acceleration score are reported and average within the three drop test cases, Lateral, Pitched and Backward.

PS	Lateral	Pitched	Backward	Average PS value
A1	-27,34	20,54	-58,78	-21,86
A2	31,48	79,13	43,29	51,30
A3	30,94	72,50	50,24	51,23
B1	-47,17	24,46	-61,83	-28,18
B2	28,87	80,00	45,49	51,45

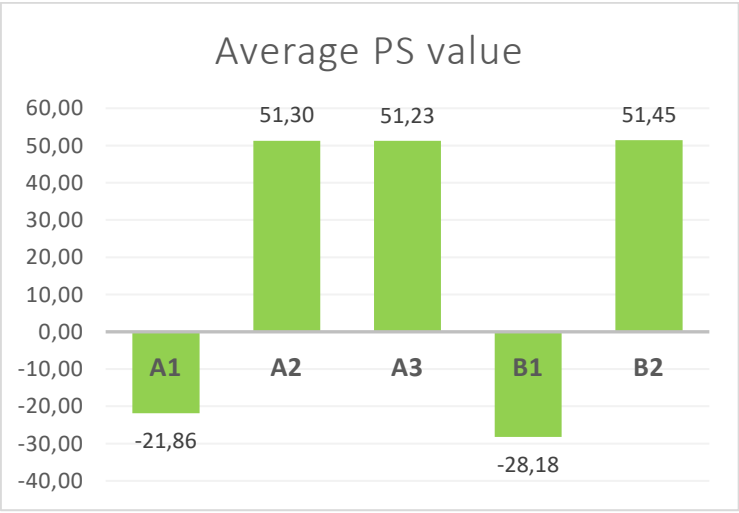

FIGURE 61 AVERAGE PS VALUES

Discussion

The simulation overestimates the experimental peak values for the translational accelerations, and rotational accelerations, while the predicition of the rotational velocity is in general acceptable with correlation coefficients up to 95%.

While the correlation coefficients are in some cases (A2,A3,B2) acceptable or almost acceptable, the peak linear acceleration scores are indicating a poor correlation, especially for the "fitted" configurations (A1,B1) that show a stiffer response with respect to the experimental values, determining a negative PS value for both the fitted configuration. The only values that are reasonable, although not considerable acceptable to state that the model is validated, are the one for the configurations A2, A3 and B2 with similar averaged values for the PS (50%).

The similar performance of the A2, A3 and B2 configuration suggest that the material model is not much influent (if reasonable for the application), if the data of input are the same. In absence of data to be implemented it can be reasonable to use a material model without strain rate effect, in this case the input curve was the one corresponding to strain rate 100 s^{-1}.

The material properties are obtained from detailed analysis carried out on EPP samples that are not directly taken from the helmet. This could be issued as one of the causes of unrealistic behavior of the model. However, some compression curves from the original helmet EPP were available and compared with the one obtained in this work, and for the same strain rates very small differences are present.

The material model 083 has been tuned for shear and compression, and the numerical response shows a small difference in the shear behavior, that determine a more compliant shear response in the elastic range for the EPP with respect to the real one.

The material 083 was also tested with the option of linear elastic response in tension and cutoff stress of 1 MPa, close to the experimental values. The comparison between configuration A2 and A3 show small differences, and although the model is not completely validated it is possible to state that paying

attention to set the tensile cut-off correctly a good approximation can be made in absence of the possibility to specifically tune the shear response of the material, for what concern oblique impact simulations.

The influence of the fitting is the most relevant aspect: the fitted configuration, compared with one where the helmet is scaled of 2% and 3% in width and length, shows an increase in the translational acceleration estimation that is of the order of more than 50 g. The Peak Linear Acceleration Score for the "fitted" configurations is often negative, as confirm that the procedure must be refined. Since it was not possible to participate at the experiment, it is possible that the head form and helmet were differently fitted together, so the fitting is accountable as one of the cause of the poor similarity between FEM and experimental data. A a methodic system to monitor the fitting in the experimental tests (contact pressures) could be an interesting development to collect information and control this variable during test sessions.

An observation could be extended to real life application, where the fitting of the helmet is confirmed to be a critical factor for the effectiveness in protecting from traumatic brain injuries.

The eventuality of damage in the drop impact test is not taken into account in the present FE model, although it is not frequent and will probably not change much, it is possible that additional dissipation mechanism, other than deformation intervene in the process.

How the liner is attached to the shell is an important factor, the fact that the FE presents as assumption an uniformly attached liner is in contrast with the possibility that the two parts could share only a certain number of spot where are glued. The failure of the bond between shell and liner is a possible future improvement to add, following the dissection of a sample helmet.

The data filtering has a relevant impact on the comparison between the experimental and FEM results, and although it is not the main source of error, a more detailed report is needed from the experimental data.

Innovation in helmet design for improved protection against rotational kinematics

Following the research on the biomechanical aspects of head impact and traumatic brain injury, innovations have been introduced in the helmet design and testing process.

Some innovative helmet construction configuration have been defined to better protect the brain taking into account the rotational kinematic of the head during impact.

At present, the majority of helmet test standards for the several typologies doesn't consider angular kinematics even if in some cases oblique impact test is performed. Probably in the future the certification procedures will involve a rotational acceleration (and angular velocity) related criterion to assess the effectiveness of the protective device.

Helmet manufacturers and academical researchers are developing helmet and components to ensure a better protection against impacts involving oblique contact. Some concepts are more effective than others and the difference in the industrialization is relevant, as in certain cases the additional protection is provided with an additional component fitted to an existing helmet, in other a completely new design process must be made.

AIM (Angular Impact Mitigation) system and aluminum Honeycomb liner (Hansen et. Al. [25])

A prototype was developed in 2012

The study consisted in the comparison of the acceleration, angular and translational, between two helmet concepts.

In the control one the structure is composed by the outer shell (ABS, 3mm thick), foam liner (EPS, 85 kg/m^3,17 mm thick) and comfort padding in PU foam.

In the modified one, the structure comprises a 17 mm aluminum honeycomb liner instead of the EPS. The inner PU comfort foam is kept.

The mass of the two was equivalent (408 g)

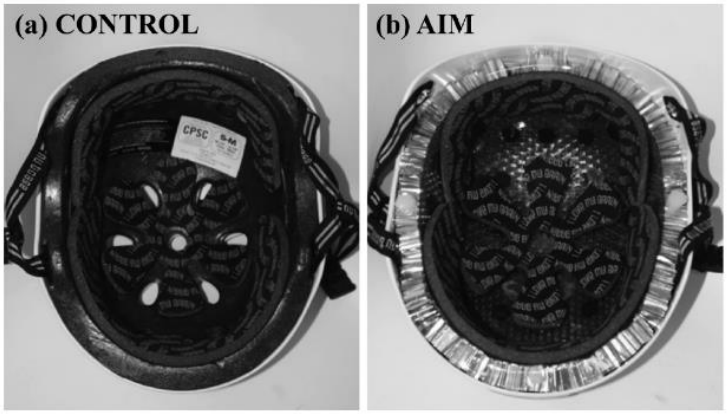

FIGURE 62 MODIFICATION OF THE HELMET WITH HONEYCOMB LINER

The normal impact test (6.2 m/s, flat anvil) showed a 14% linear acceleration reduction for the AIM helmet.

The oblique impact test (4.8 m/s, 30° inclined anvil) showed a 34% reduction in the rotational acceleration peak value.

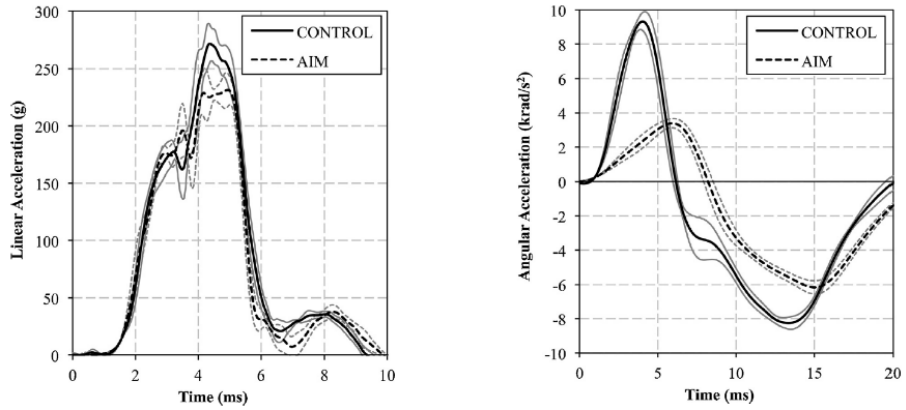

FIGURE 63 REDUCTION IN THE ACCELERATION WITH AIM SYSTEM

Since the tests were performed with a HIII head-neck model, also the forces on the neck were monitored, and showed a reduction of 32%,25% and 22% respectively for Max neck shear, Max neck compression and Max neck moment.

Other prototypes were made, showing that good results can be obtained with hybrid Honeycomb-Expanded polymer liners, as written by Caserta (2012).

One of the drawback of this construction method is the manufacturing that significantly differ from a classic EPP or EPS helmet liner.

MIPS Multidirectional Impact Protection System (available on market) [26]

MIPS is a patented protection system, that was developed in Sweden, starting in 1996. Following several concepts, each one based on the intuition that a reduction of the rotational kinematics parameters that are transferred to the head is achievable with the interposition of a low friction layer inside the helmet. The first prototypes were based on the interposition of a thin layer between the shock absorbing liner and the helmet shell. At present, MIPS AB (SE) have a wide proposals range spacing from strips of low friction material to be interposed between the comfort pads and foam to cap-like shells to be interposed between comfort pad and foam liner, or textile inserts including a low friction layer.

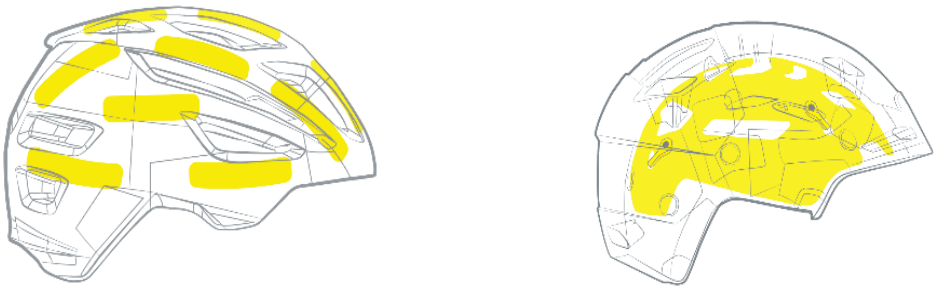

FIGURE 64 MIPS IN DIFFERENT CONFIGURATIONS

The use of combined oblique drop tests and FE modeling using a detailed FE model of the human head supports the claim that the adoption of a MIPS system reduce the axonal strain, leading to an higher level of protection.

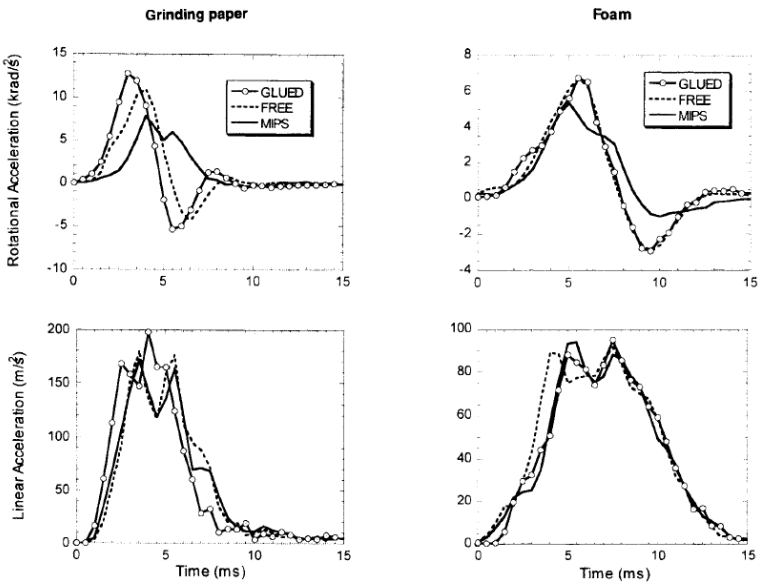

FIGURE 65 ROTATIONAL ACCELERATION

MIPS AB is not a helmet manufacturer but provide the MIPS product to the helmet manufacturers that choose to add this element to their model.

From the industrial/commercial point of view the minimal impact on the design and the possibility to adapt existing helmets design is an important advantage that is guaranteeing commercial success. In terms of user perception, the easily explanation of the involved damaging/protection mechanism, with the use of clear graphic support, and the research encouragement to put effort in managing the rotational kinematics during impact provide a good base for the marketing operations.

6d helmet [27]

6D Helmet is a helmet manufacturer that have a patented innovative protection system called Omni Directional System (ODS).

The ODS helmet are made by a liner split in two concentric shells, in the between a suspension system is realized by mean of elastic hourglass shaped dampeners.

This system allows the two EPS liners to move in the radial and tangential direction, ensuring a reduction of the acceleration that are transmitted to the brain.

FIGURE 66 6D HELMET SYSTEM

This system is 6D Helmets proprietary and based on custom designed helmets. The shells are conveniently shaped to guarantee a good fit on the head, an at the same time the clearance and the spherical shape of the two parts avoid the risk of "shape locking".

Independent third part tests proven the system to be effective in the reduction of the acceleration transmitted to the brain.

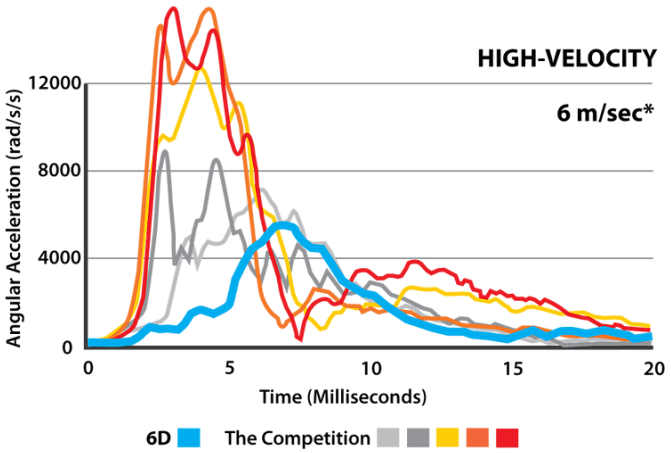

FIGURE 67 ANGULAR ACCELERATION REDUCTION WITH 6D SYSTEM

The helmets model and prototypes presented are only a portion of all the ones developed during the years, however they provide a good representation of the strategies adopted to limit the rotational accelerations transmitted to the brain.

Another alternative is the one with a low friction layer on the outer shell contact surface, the principle is the same presented by MIPS.

General design good practices

A consistent design of the outer shell is important to provide a smooth sliding on the contact surface. Avoidance of shapes and bosses that can interfere with the sliding between contacting surfaces is to avoid.

Conclusions

A modified shear test rig is designed and tested with different foams. The rig has proven to be suitable for the testing of foams of different characteristics. The simple design allows an easy manufacturing and the realization of multiple set of plates, allowing the user to perform multiple tests in less time, considering that the epoxy glue require to be cured for 24 hrs. A drawback of this method is the fact that it's not a completely pure shear or a completely simple shear test, so the validation via FE modeling must be made against simulation of the actual test. A Digital Image Correlation (DIC) technique can be helpful to furtherly investigate on the actual strain state in the specimen.

A detailed and compression-shear validated material model for the EPP foam of nominal density 50 Kg/m^3 is developed. Although it can be possible to improve the model with dynamic drop tests and the use of dedicated software to better fit the material response (LS-Opt).

The material model, together with the ABS properties are input for the FE model of the Easton 380. No penetration of the nodes is evident from the tests and three oblique test configurations are presented, with the helmet fitted and the stress in the foam initialized.

The level of reliability of the simulation is not significantly increased from the one achieved in 2017 by I. Rigoni, as a confirm of the value of her work.

A model of the fitted FE helmet with the possiblity to initialize the stress state in the liner is generated and the files organized in a hierarchic structure to be available for the use.

A major improvement in the modeling procedure can be to proceed with separate modeling and validation of the components. This require a certain quantity of helmet samples and dedicated instrumentation.

An improved procedure can be the one following

1. Experimental test:
    i. Drop tests with marked orientation and impact location. It is important to have a trigger system in order to precisely replicate the experiment via FE analysis.
2. Material test:
    i. EPP material test: Compression, Tension, Shear, Drop test
    ii. Comparison of properties between EPP extracted from helmet samples and spare EPP of equal density. If different proceed with the characterization on the helmet EPP sample. If not possible for the shear test because of the specimen size, proceed with equal density EPP.
3. Component test
    i. Choice of a loading condition for the bare shell, and for eventual removable padding. For example, compression of the shell across the diameter and compression of a foam pad as it is extracted from the helmet
4. Evaluation of the liner-shell constraint system
5. FE modeling
    i. Shell FE modeling and validation against component test
    ii. Foam material modeling and validation against compression and drop test
    iii. Foam validation against shear test
    iv. Eventual another components validation
6. Complete FE model validation and troubleshooting (contact, etc.…)

As conclusion, it can be stated that the topic of protection against Traumatic Brain Injury is constantly an area of investigation for the researchers. During the period of development of this work at KTH it was possible to participate and gain comprehension of the state of art in the subject, and appreciate innovative research framework aimed at the comprehension of brain injury mechanism and accident reconstruction via FE analysis.

Appendix A Head Injury Criterions

In the following some of the principal criterions for assessing the risk of brain injury are presented.

HIC

For obvious reason the research on head impact biomechanics cannot be conducted by mean of in-vivo experiment on human head but using an instrumented dummy or FE modeling. In vehicle safety assessment acceleration values from instrumented Free Motion Head form (FMH) located in the vehicle during crash tests are used to evaluate the level of protection offered to the passengers. To analyze and compare experimental data it is necessary to make use of standardized parameters that can predict the likelihood of a brain injury from the kinetic and dynamic parameter of the head.

One of these is the Head Injury Criterions (HIC) and are based on the translational acceleration that the head experiences during the impact time.

The expression for the HIC is

$$HIC = \left\{ \left[\frac{1}{t_2 - t_1} \int_{t_1}^{t_2} a(t)dt \right]^{2.5} (t_2 - t_1) \right\}_{max}$$

EQUATION 8 HEAD INJURY CRITERION

Where (t_2-t_1) must be max 36 ms. The usual values are 15 and 36 ms.

The HIC considers the acceleration peak and the exposure time as factors enhancing the probability of a MTBI to occur.

Reference values can be found from the NHTSA rating, as HIC-15ms of 700 is the maximum allowed to obtain an *acceptable* rating in the Insurance Institute for Highway Safety (IIHS) and to respect the provisions of NHTSA. A level of 700 is associated with a 5% risk of severe head injury, while a value of 1000 is associated with a 18% probability of severe head injury and a 9% probability of moderate head injury.

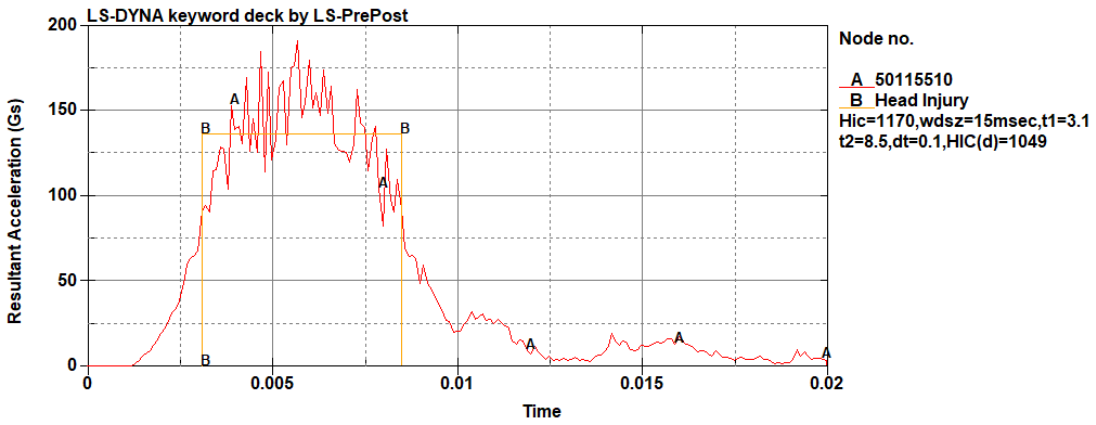

FIGURE 68 HIC CALCULATION IN FE ANALYSIS

Regarding the rotational acceleration, some observations were made

BrIC Brain Injury Criterion [28]

The BrIC is a kinematically based criterion, that refer to the rotational kinematics of the head. It is based on correlation studies between animal experiment, FE simulations, on field measurement and epidemiological evidences in football players.

The BrIC risk curves are developed in a Weibull form, and are available for different severities of brain injury.

The study state that there is correlation between the rotational velocity caused by the impact, and the direction of rotation is influent. To be specific, the injury thresholds are different for rotation about the different reference axis of the head. The final expression for the BrIC is

$$\mathrm{BrIC} = \sqrt{\left(\frac{\omega_x}{\omega_{xcrit}}\right)^2 + \left(\frac{\omega_y}{\omega_{ycrit}}\right)^2 + \left(\frac{\omega_z}{\omega_{zcrit}}\right)^2}$$

EQUATION 9 BRIC

The values for $\omega_{xcrit}, \omega_{ycrit}, \omega_{zcrit}$ for a certain degree of brain injury severity are established referring to the risk of an injury of the same risk as predicted by the Cumulative Strain Damage Measure (CSDM) and Maximum Principal Strain (MPS) that are in turn related with the rotational velocity, and so to the BrIC.

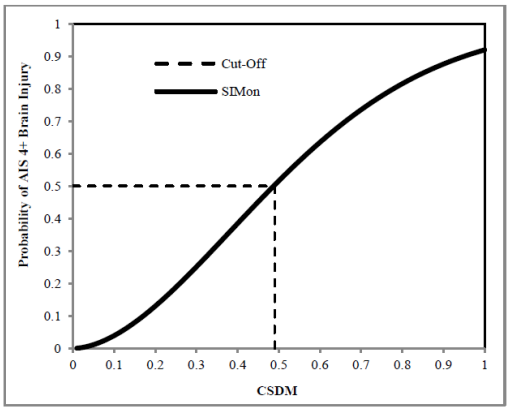

FIGURE 69 CUMULATIVE STRAIN AND INJURY RELATION (TAKHOUNTS ET AL. 2013)

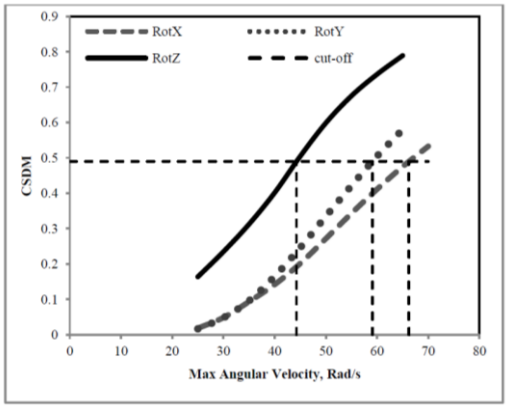

FIGURE 70 MAX ANGULAR VELOCITIES AND CSDM (TAKHOUNTS ET AL. 2013)

TABLE 24 CRITICAL ANGULAR VELOCITIES FOR DIFFERENT AXIS

Critical Max Angular Velocity	Rad/s (CSDM Based)	Rad/s (MPS Based)	Rad/s (Average of CSDM and MPS)
ω_x	66.20	66.30	66.25
ω_y	59.10	53.80	56.45
ω_z	44.25	41.50	42.87

WSTC Waine State Tolerance Curve

The WSTC criterion is based on the onset of skull fracture, which is thought to be correlated with the occurrence of brain injury. This study put the base from which the other criterions were derived, considering the influence of both the peak value and duration in time of the acceleration. The area below the curve correspond to combinations Time-Acceleration that are not causing skull fracture.

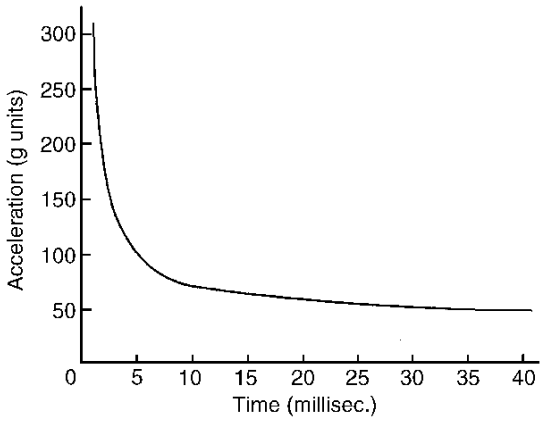

FIGURE 71 WAINE STATE TOLERANCE CURVE

GAMBIT (Generalised Acceleration Model for Brain Injury Threshold) [29]

The GAMBIT criterion is derived from the mechanical considerations applied to complex stress states where an "equivalent" stress state is defined to be compared with the material properties. In the GAMBIT criterion the translational and rotational accelerations are treated like stresses and are combined in a form that is generalized as:

$$G(t) = \left[\left(\frac{a(t)}{a_c}\right)^n + \left(\frac{\alpha(t)}{\alpha_c}\right)^m\right]^{\frac{1}{S}}$$

EQUATION 10 GAMBIT CRITERION

Where:

- a(t) and α(t) are the translational and rotational accelerations
- n,m,s are constants to be defined in order to fit the experimental data
- a_c and α_c are the critical values for a(t) and α(t)

The n,m,s coefficients can be simply assumed to be equal to 1, so the criterion assumes the form of a linear weighting (G1), or assuming n,m,s=2 an elliptical "failure" surface is described [29].

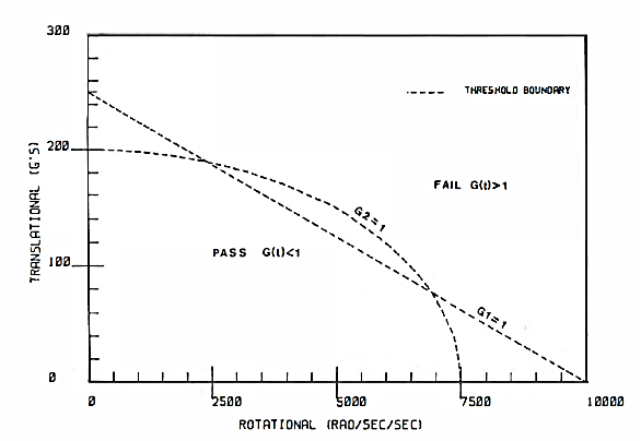

FIGURE 72 GAMBIT GRITERION ENVELOPES

References

[1] I. Rigoni, “FE-Modelling and Material Characterization of Ice-Hockey Helmet,” 2017.

[2] W. N. Hardy, “Correlation of an FE Model of the Human Head with Local Brain Motion--Consequences for Injury Prediction .,” no. October, 2015.

[3] S. Kleiven, “Finite Element Modeling of the Human Head,” *Med. Biol. …*, vol. 12, no. 1, pp. 14–21, 2002.

[4] M. Fahlstedt, P. Halldin, and S. Kleiven, “The protective effect of a helmet in three bicycle accidents - A finite element study,” *Accid. Anal. Prev.*, vol. 91, pp. 135–143, 2016.

[5] *Mechanism of Concussion in Sports*. 2018.

[6] C. Giordano and S. Kleiven, “Evaluation of Axonal Strain as a Predictor for Mild Traumatic Brain Injuries Using Finite Element Modeling,” *Stapp Car Crash J.*, vol. 58, no. 14, 2014.

[7] J. T. Barth, J. R. Freeman, D. K. Broshek, and R. N. Varney, “Acceleration-Deceleration Sport-Related Concussion: The Gravity of It All,” *J. Athl. Train.*, vol. 36, no. 3, pp. 253–256, 2001.

[8] ASTM, “F1045-16 Standard Performance Specification for Ice Hockey Helmets,” *Current*, pp. 1–10, 2016.

[9] S. Christian and C. Lon, “A new helmet testing method to assess potential damages in the Brain and the head due to rotational energy,” 2014.

[10] D. S. Liu, C. Y. Chang, C. M. Fan, and S. L. Hsu, “Influence of environmental factors on energy absorption degradation of polystyrene foam in protective helmets,” *Eng. Fail. Anal.*, vol. 10, no. 5, pp. 581–591, 2003.

[11] “matlab help.”

[12] H. T. Designed, “E3000 All-Electric Dynamic Test Instrument Hardware and Software Interfaces Designed to Put You in Control A High Level of Versatility,” pp. 2–3.

[13] S. T. Method, “Standard Test Method for Compressive Properties of Rigid Cellular Plastics 1,” pp. 4–8, 2018.

[14] A. Hirth, D. Ag, S. Matthaei, and D. Ag, “Modelling of Foams using MAT83 – Preparation and Authors : Correspondence :,” no. 0, pp. 59–72.

[15] K. Kanny, H. Mahfuz, T. Thomas, and S. Jeelani, “Static and Dynamic Characterization of Polymer Foams Under Shear Loads,” *J. Compos. Mater.*, vol. 38, no. 8, pp. 629–639, 2004.

[16] K. VandenBosche, J. Ivens, I. Verpoest, J. Goffin, G. Van der Perre, and J. Vander Sloten, “Combination Shear-Compression Testing of Foam Materials for Their Application in Bicycle Helmets or Other Complexly Loaded Structures,” *18th Int. Conf. Compos. Mater. 27-31 July, 2009, Edinburgh, Scotl.*, pp. 4–9, 2009.

[17] B. Croop, H. Lobo, and N. DatapointLabs, “Selecting material models for the simulation of foams in LS-DYNA,” *Proc. 7 th LS-DYNA …*, 2009.

[18] “LSTC.” [Online]. Available: www.lstc.com.

[19] “Review of Solid Element Formulations in LS-DYNA,” 2011.

[20] “d3view.” [Online]. Available: www.d3view.com.

[21] G. Milne, C. Deck, N. Bourdet, R. P. Carreira, Q. Allinne, and A. Gallego, “Bicycle helmet modelling and validation under linear and tangential impacts,” *Int. J. Crashworthiness*, vol. 19, no. 4, pp. 323–333, 2014.

[22] A. Trotta, A. Ní Annaidh, R. O. Burek, B. Pelgrims, and J. Ivens, “Evaluation of the head-helmet sliding properties in an impact test,” *J. Biomech.*, vol. 75, pp. 28–34, 2018.

[23] V. Bewick, L. Cheek, and J. Ball, “Statistics review 7: Correlation and regression,” *Crit. Care*, vol. 7, no. 6, pp. 451–459, 2003.

[24] E. G. Takhounts, M. J. Craig, K. Moorhouse, and J. Mcfadden, “Development of Brain Injury Criteria (BrIC),” vol. 57, no. November, pp. 243–266, 2013.

[25] J. A. Newman, “A Generalized Model for Brain Injury Threshold,” *Proc. Int. Conf. Biomech. Impact, 1986 (pp. 121-131).*, pp. 121–131, 1986.

[26] K. Hansen *et al.*, “Angular Impact Mitigation system for bicycle helmets to reduce head acceleration and risk of traumatic brain injury,” *Accid. Anal. Prev.*, vol. 59, pp. 109–117, 2013.

[27] “MIPS protection.” [Online]. Available: www.mipsprotection.com. [Accessed: 27-Jun-2018].

[28] “6D helmets.” [Online]. Available: https://www.6dhelmets.com/innovation/.